Technical University Braunschweig

Faculty of Civil Engineering

Leichtweiss – Institute for Hydraulic Engineering

Section of Hydromechanics and Coastal Engineering
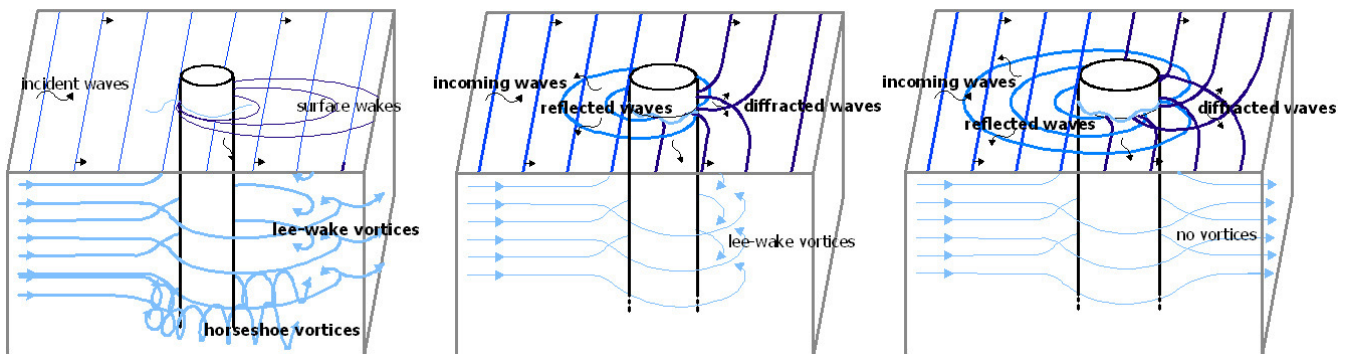
Delft University of Technology

Faculty of Civil Engineering and Geosciences

Section of Hydraulic Engineering

Predictability of Scour at Large Piles
due to Waves and Currents

Diploma Thesis

Author: Regina Haddorp

(Student No.: 2561989)

Delft, July 2005

Preface

This thesis forms the completion of my studies at the Technical University of Braunschweig, Faculty of Civil Engineering, in Germany. At the TU Braunschweig I specialized in Coastal Engineering, Structural Analysis and Technical Building Equipment. By the Erasmus-Sokrates-Program and the University of Technology in Delft I have been enabled to improve my knowledge in the field of Offshore Technology and Offshore Wind Energy.

Participating the lecture "Offshore Wind Farm Design" in Delft I learned about the uncertainties in scour prediction around offshore wind turbines and its possible consequences: Observing the design rules, the dictated scour hole varied between 4 and 6 meters, while the size of the scour is an important cost parameter. Extra steel for the strengthening of the turbine or providing of scour protection costs millions of euros for a wind farm. More than one hundred wind farms are currently planned only in Europe.

I got interested in this topic and it fitted well with my fields of study. In Ir. H.J. Verhagen, Ir. J. Olthof and Prof. Dr. Ir. M.J.F. Stive from the section of Hydraulic Engineering at the University of Technology in Delft. I found tutors who were interested as well as willing to guide me. The differences in the scour processes between slender and large piles have been chosen to serve as starting point. At my home institution the tutors Prof. Dr. Ir. H. Oumeraci and Ir. M. Brühl accepted this project as my diploma thesis.

I enjoyed my studies on the scour around large piles, not only because I like to deal with the combination of wave flow and structures, but also for the reason that the utilising of the insights in the scour processes is from use to the society. An overestimation of the scour depth could cause the waste of funds or the rejection of projects, while an underestimation can lead to the failure of structures.

Since this project runs for only 13 weeks the results might not go as far as desired, nevertheless a good insight in the state of the art is presented and important conclusions and recommendations are made.

I thank my coordinators Prof. Stive, Mr. Verhagen and Mr. Olthof for supporting and guiding me with my project at the University of Technology in Delft as well as I thank Prof. Oumeraci and Mr. Brühl for supporting me from the Technical University of Braunschweig and permitting me to write my final thesis abroad.

I would not have managed my studies and entire education without psychological support. For providing this together with faith and love I thank my mother, my friend Miriam Dittmer and my partner Richard Lohman. Thanks also to Richards father who corrected my English and encouraged me by his interest.

<div align="right">

Delft, July 2005
Regina Haddorp

</div>

Abstract

Installing a structure offshore interferes with the existing flow conditions? The wave and current induced velocities are locally heightened and therewith sediment is lifted and washed away. A so-called scour hole, a deepened area around the structure, is formed.

In the design of an offshore wind turbine the formation of a scour hole needs to be considered or scour protection must be provided. Design rules dictate a design scour depth of one to two times the diameter of the pile. The piles of offshore wind turbines are at least 3.5 meter wide, so that the predicted scour depth differs in a size of 3.5 meter or more. The average scour depth is much smaller.

Most of the knowledge about scouring at piles is referred to relative slender piles. If water particles move far compared to the width of the pile the flow separates and vortices are formed. These vortices are known as the main causes of scour. At large piles however, the flow does not separate. Instead the wave field is transformed by reflection and diffraction. Therewith the relative scour depth around large piles is much smaller than at small piles.

Basing on this understanding the predictability of scour around monopile-founded wind turbines is analysed. Three flow regimes are characterized and defined in dependency of the Keulegan-Carpenter number. This is explained in Section 2.1 and applied to offshore wind turbines in Section 5.2. Evaluating scour the flow characteristics, the sediment transport and the stability in relation to the foundation need to be considered. An insight into the most important aspects of scour development is given in Chapter 2. Scouring around slender piles has been widely investigated. Important determinations related to offshore installed piles are summarized in Chapter 3.

Scouring around large piles is not understood in detail. Based on the review of insights in flow characteristics, empirical and analytical approaches scour around large piles is discussed in Chapter 4.

Under consideration of uncertainties, which are explained in Section 5.2, the knowledge of flow regimes and maximal scour depths are applied to offshore wind turbines and the design of scour protections in Section 5.3 and 5.4.

The application to offshore wind turbines shows that under moderate wave conditions the depth of the scour hole around a pile is less than thirty percent of its diameter. However, under extreme wave conditions, which are expected less than once a year, the scour hole can increase up to a limit of 1 time of the diameter. According to current design standards, even scour depth of 1.5 and 2 times of the diameter may occur. This effect a more than five times too large considered impact of scouring in the fatigue analysis of offshore wind turbines.

Investigation of scouring processes leads to a better insight and with this knowledge one can reduce the uncertainties and thereby decrease the "best practice" safety factors.

Table of Contents

Appendices:

   Appendix A: Definition of Parameters

   Appendix B: Definition of the Boundary Layer

   Appendix C: Equilibrium Scour hole at large piles by Sumer and Fredsøe (2001b)

   Appendix D: MacCamy and Fuchs theory

   Appendix E: Confrontation of the prediction and in field measurements

   Appendix F: Example Application to Offshore Wind Turbines

List of Figures

List of Tables

List of Symbols

Symbol	Definition	Unit
a	amplitude of the orbital motion	[m]
A_D	exposed surface area due to drag force or	$[m^2]$
A_L	exposed surface area due to lift force	$[m^2]$
C_D	drag coefficient	[-]
C_M	Shape coefficient due to inertia force	[-]
D	pile diameter	[m]
$^D/_L$	diffraction coefficient	[-]
E	modulus of elasticity	$[N/m^2]$
f. f_1	natural frequency	[1/s]
F_d	lift force	[N]
F_g	gravity force	[N]
F_i	inertia force	[N]
F_l	lift force	[N]
Fr	Froude number	[-]
f_w	wave friction coefficient	[-]
d	average grain diameter	[m]
d_{50}	median grain diameter	[m]
g	acceleration of gravity	$[m/s^2]$
H	wave height	[m]
H_{max}	maximal wave height	[m]
h	water depth	[m]
$(H/L)_{max}$	maximal steepness of waves	[-]
k	wave number	[1/m]
k_s	bed roughness length	[m]
KC	Keulegan-Carpenter number	[-]
L	wave length	[m]
L_M	length in the model	[m]
L_N	length in the nature	[m]

Symbol	Definition	Unit
l	lever	[m]
M	shear stress amplification factor due to presence of structure	[-]
m	mass (Chapter 2)	[kg]
m	wave form coefficient (Chapter 3)	[-]
N	number of load cycles	[-]
O()	order of	[-]
q	volumetric net sand transport rate	[m^3 s/m]
q_S	Sediment transportation rate per unit time	[m^3/s]
$\partial qs/\partial x$, $\partial qs/\partial y$	flux of sediment passing through unit of length	[m^3/ms]
Re	Reynolds number	[-]
Re_D	Reynolds number of the pile	[-]
Re_δ	Reynolds number of the bottom boundary layer	[-]
Re_*	particle Reynolds number	[-]
S	equilibrium scour depth	[m]
S/D	relative scour depth	[-]
T	wave period	[s]
T_N	Measure of time in the nature	[s]
T_M	Measure of time in the model	[s]
T_S	characteristic time-scale	[s]
T*	dimensionless time-scale	[-]
t	wall thickness (Section 2.3)	[m]
t	time (Chapter 3, 4)	[s]
U	Ursell parameter	[-]
u	free-stream velocity of the current	[m/s]
u_b	near bed velocity	[m/s
u_c	(depth-integrated) current velocity	[m/s]
u_{cw}	velocity ratio of current and waves	[-]
u_m	maximal orbital velocity at the sea-bed	[m/s]
u_{*c}	critical shear velocity	[m/s]
V	volume of the sediment grain	[m^3]
z	vertical coordinate, z = 0: surface of the sea	[m]

Symbol	Definition	Unit
β	pivoting angle	[°]
Δ	relative density	[-]
δ	thickness of the boundary layer	[m]
δ^*	displacement thickness of the undisturbed bottom boundary flow	[m]
ε	bed porosity	[-]
λ_υ	void ratio of sediment	[-]
λ_T	scale factor of time	[-]
λ_L	scale factor of lengths	[-]
ν	viscosity of the fluid	[-]
ρ, ρ_w	density of the water	[kg/m^3]
ρ_S	density of the sediment grain	[kg/m^3]
σ_{amp}	Stress amplitude of load cycle	[N/m^2]
σ_N	normal stress	[N/m^2]
τ	shear stress	[N/m^2]
τ_C	critical shear stress	[N/m^2]
τ_w	bed shear stress due to cyclic (wave) loading	[N/m^2]
τ_0	ambient bed shear stress	[N/m^2]
ω	wave frequency	[1/s]
ψ	Shields parameter	[-]
ψ_c	critical Shields parameter	[-]
ψ_m	momentary Shields parameter	[-]
$\partial \zeta/\partial t$	changing of elevation over time	[m/s]
∇_D	sediment deposition	[m^3/ms]
∇_E	sediment entrainment	[m^3/ms]

1   Introduction

1.1   Objectives and Motivation

Background:

Our desired standard of living includes the usage of energy at a high level. The availability of our main and cheapest resources, oil and gas, decreases and their production becomes more difficult and expensive. Conflicts over the remaining oil reservoirs have occurred. There is a strong need to develop alternative energy sources.

Wind energy is an up-and-coming alternative. By producing one kilowatt hour for € 0.03 to € 0.08 (Zaaijer, 2004a; Cockerill et al., 1997) it is as expensive as nuclear energy without its potential danger. Since 1990 wind turbines are installed offshore. This decreases the disadvantages of noise exposure and landscape defacement and increases the efficiency through better wind conditions and larger wind farms.

The installation of a structure offshore leads to new difficulties: The structure creates flow disturbances which can lead to erosion in the vicinity of the structure. Since the erosion decreases the stability of the wind turbine, design rules dictate to consider a scour hole of 1.0 to 1.5 times the diameter of the pile. Designing a monopile founded wind turbine with the current design rules the installation of a scour protection is mostly more economic than elongating and strengthening the pile.

Motivation:

As mapped in Figure 1-1, 15 000 offshore wind turbines are to be erected in the next 15 years.

2020: around 200 wind farm including **15 000 turbines**
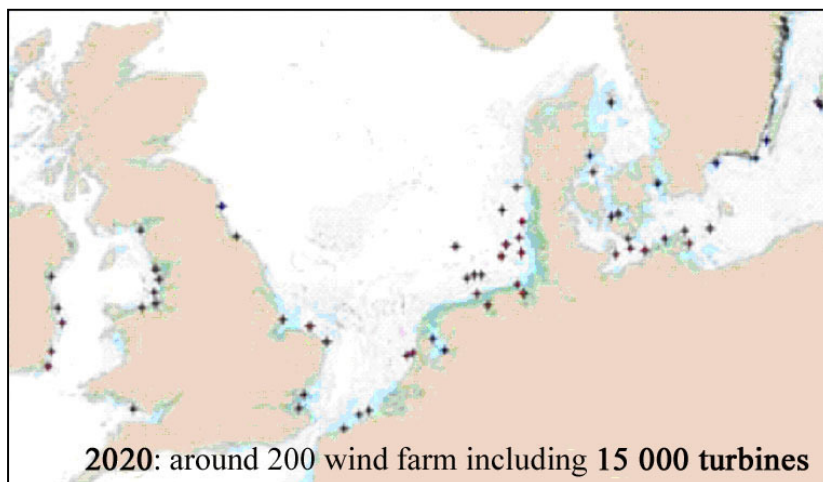
Figure 1-1: Planned wind farms in Europe (according to Zaaijer, 2004a)

The installation of scour protection around the foundation pile of a wind turbine costs between € 150.000 and € 300.000 (Tempel et al., 2004; Van der Oord ACZ, 2003), so that about 3 billion euros need to be spent on scour protection for the planned projects in Europe. To reduce these costs research projects are running to improve scour protection methods and develop new alternatives.

This thesis analysis a different approach: Comparing the estimated scour depth of design codes with field measurements there are noticeable discrepancies. An illustration is given in Figure 1-2. For foundation piles of offshore wind turbines common diameters are 3.5 to

4.5 meters. A development to suction piles with diameters of 6 meters and more is currently carried out. Therefore the discrepancies in the design rules further increase.
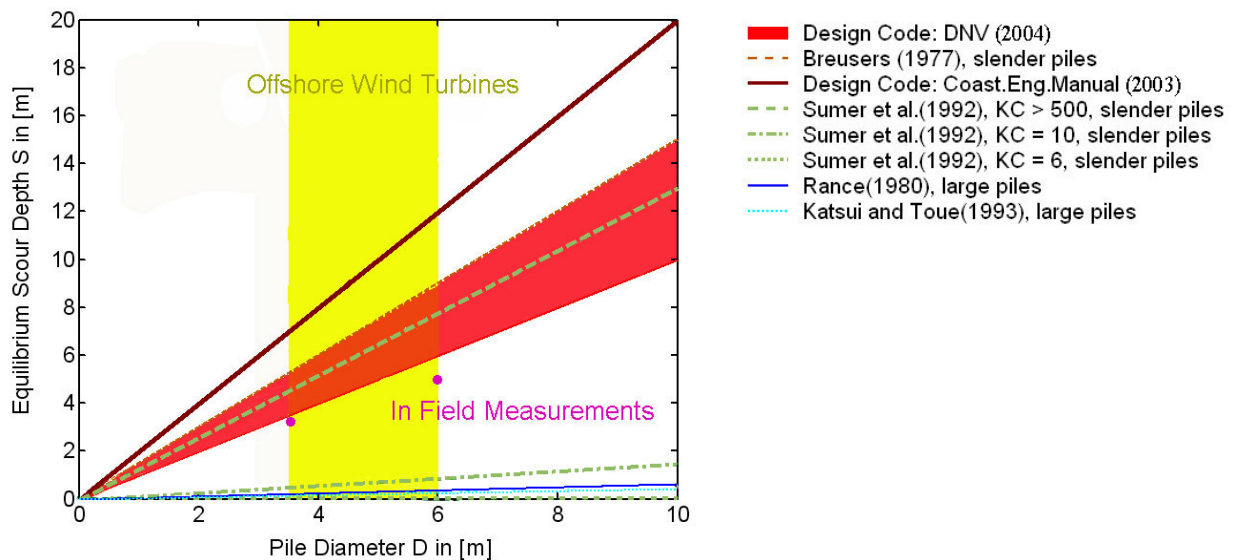
Figure 1-2: Confrontation of design codes (red), new insight in large piles (blue) and
in field measurements after storms (magenta)

Research over the last decade on piles with large diameters revealed that the scour process around slender and large piles is basically different. The design rules ensure the maximal scour depth to be linearly dependent on the pile diameter. The ratio of the maximal scour depth to the pile diameter is much smaller at "large piles" (Figure 1-2: blue lines) than at slender piles (green lines). The field measurements at two prototype piles (magenta) are between the prediction of slender piles and large piles.

Objectives:

To avoid an un-economic design of the wind turbine and the scour protection, it is important to evaluate the new understanding of scour processes on the foundation piles of offshore wind turbines. In this thesis the scour processes at offshore wind turbines are clarified and the predicted scour depths by design rules are checked. Conclusions are drawn for the design of offshore wind turbines and the application and design of scour protection. Recommendations for further research in the field of scouring and scour protection are finally drawn up.

The most important steps are:
- Analysis of flow characteristics and hereon the definition of flow regimes (Section 2.1) and classification of offshore wind turbines according to these flow regimes
- Review of the scour processes at slender piles (Chapter 3) and analysis of scour predictability at large piles (Chapter 4)
- Prediction of scouring around offshore wind turbines (Section 5.3) under evaluation uncertainties in scour development parameters (Section 5.2)
- Possibility and usefulness of considering the modification of the scour hole over the life-time in the fatigue analysis of the pile (Section 5.3)

1.2 Methodology and Content of the thesis

At common offshore piles, the scour development is mainly caused by vortices which are induced by flow separation. The occurrences of these vortices depend on the motion of water particles in relation to the size of the structure. Large piles do not cause noticeable vortices, instead the influence of diffraction is significant. Consequentially three flow regimes are defined (Section 2.1), namely the slender-pile flow regime (dominated by vortices), the diffraction regime (dominated by diffraction and reflection) and the intermediate flow regime (also dominated by diffraction and reflection but influenced by lee-wake vortices). Background information about flow characteristics, sediment transportation and the stability of the wind turbine are given in Chapter 2.

The flow regime around slender piles has been well investigated. Approved formulae, which are useful for the discussions and conclusions (Chapter 5,6), are summarized in Chapter 3.

In Chapter 4 the flow regime and scouring around large piles are analysed. Reviewing relevant reports in this field, the knowledge about the flow characteristics is summarized and analysed in Section 4.1. Attempts of the empirical evaluations are introduced and appraised under consideration of experimental results and theoretical coherences in Section 4.2. To get a complete overview about the state of the art, theoretical approaches and further influences are discussed in Section 4.3.

The maximum scour depth is predicted under moderate and extreme wave conditions by analysing the data of offshore wind farm projects with respect to the defined flow regimes. In Chapter 5 the predictability of scouring is discussed. More over the reasons for the consideration of the modification of the scour hole during its life-time in the fatigue analysis are discussed.

Chapter 6 summarises conclusions for the design of offshore wind turbines and scour protection. Recommendations for further research on scouring and scour protection are made.

Figure 1-3: Illustration of the content of the thesis

The composition of this report including the relations between the chapters is illustrated in Figure 1-3.

2 Background: Scour Processes around Circular Piles

Building a structure in the marine environment interferes with the flow conditions. By causing accelerations and turbulences, the sediment transport potential is locally higher, so that more grains are lifted and washed away. The local erosion caused by a structure is called scour. For the stability of a structure, it is fundamental to consider the loss of sediment since the sea-bed needs to take on the loading. The interactions between the structure, the flow and the sediment are brought together in the flow diagram shown in Figure 2-1
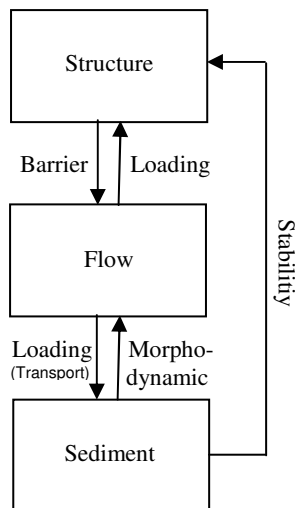
Figure 2-1: Interaction of structure, flow and sediment

In this chapter the physical background is explained since the understanding of the basic processes is required in order to draw the right conclusions. In Section 2.1 the hydrodynamic influences of the structure on the flow are introduced. The influences of the flow on the sediment are analysed in Section 2.2 and the effects of morphological changes on the structure are outlined in Section 2.3.

Three important parameters are going to be used in many cases. By the Reynolds number it can be characterised, whether a flow is laminar or turbulent. Re depends on the flow velocity, the flow surface and the viscosity of the fluid. The Keulegan-Carpenter number is a coefficient characterising the relation of the orbital velocity due to waves (or the amplitude of the wave motion) and the pile diameter. Re and KC as well as other basic parameters are explained in more detail in Appendix A. The diffraction factor is defined as coefficient of the pile diameter D to the wave length L.

2.1 Hydrodynamic Processes

Every construction which is placed in current or waves obstructs the flow of water particles. Pressure differences are generated, the flow lines contract and the water particles accelerate. Dependant on the shape and size of the structure, further disturbances like turbulences and reflection of waves occur. In the scope of this thesis only circular, vertical piles are of considered.

2.1.1   Flow characteristics around slender and large piles

Two kinds of flow regimes around circular piles are basically distinguished: In the regime of slender piles, the flow separates at the rear sides of the pile and the bed boundary layer (see Appendix B) rolls up around the bottom of the pile. These vortices are the main cause of scour at slender piles.

The second flow regime is referred to large diameter piles. In contrast to slender piles the flow does not separate and hence no vortices occur. Unlike the slender piles larger diameter piles influence the incoming waves. Reflection and diffraction occurs, which leads to an increase of the velocities and therewith scour occurs as well.

Under which conditions the mentioned disturbances occur at a circular, vertical cylinder is summarized under the following item, afterwards the two flow regimes are defined according to a relation of the wave motion and the diameter of the pile.

Flow separation: For **KC > O(1)** or **Re > 5** the flow over a surface of a circular pile separates (Sumer and Fredsøe, 2002). This originates in the different direction of the flow along the pile surface and the curve of the surface. An illustration is given in Figure 2-2.

Two conditions are given: The Keulegan-Carpenter number KC is related to wave action, the Reynolds number to the interference of a current. Offshore "wave and current" generally occur together. The flow regime is then mostly dependent on the wave conditions, thus the Keulegan-Carpenter number. The "order" symbol denotes the dependence on the Reynolds number. To understand the relevance of these two parameters explanation is given in appendix A.
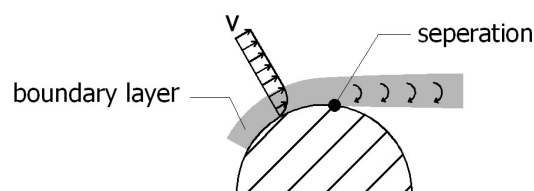
Figure 2-2: Flow separation and the formation of lee-wake vortices at slender piles

Lee-wake vortex: After the flow separates from the pile, vortices can be formed with and without vortex shedding. This is illustrated in Figure 2-3. As shown in Figure 2-2 these vortices evolve out of the unequal velocity distribution in the boundary layer at the surface of the pile.

The water particles in the lee-wake vortices hold a high amount of energy and have therewith a large influence on the morphodynamic processes.

Like flow separation, the occurrence and the kind of vortices can be described by the Keulegan-Carpenter number KC and the Reynolds number Re. The roughness of the surface also influences the lee-wake vortex. This will not be considered here.

Since lee-wake vortices occur only by separation of the flow, the same boundaries are set: **KC > O(1)** or **Re > 5**

The characteristics of the lee-wake vortices are further distinguished as indicated in Figure 2-3.

no separation

separation with Honji vortices

lee-wake vortices   vortex shedding

Current only (Sumer and Fredsøe, 1997):
Re < 5   :   no separation hence no vortices
5 < Re < 200   :   laminar vortices
Re > 300   :   turbulent
Re > 3.5 * 10^5 :   turbulent boundary layer

Waves (and Current) (Sumer and Fredsøe, 2002):
KC < O(1)   :   no separation
O(2) < KC < O(4)   :   turbulences over cylinder surface
O(4) < KC < O(6)   :   symmetry breaks up, no shedding
O(6) < KC < O(23) :   vortex shedding occurs

<u>Horseshoe vortex:</u> Analog to the lee-wake vortices the unequal velocity distribution in the bed-boundary layer can lead to rotations of the incoming boundary layer (see Figure 2-4). These vortices are called horseshoe vortices because they roll up in front and along the pile in an area shaped like a horseshoe. Due to pressure differences an up- and down flow is generated next to the horseshoe vortices. The shape of the horseshoe vortices as well as the form of the vertical flows can be seen in Figure 2-7.

In a steady streaming Sumer and Fredsøe (2002) establish the following boundaries for the occurrence of the horseshoe vortices:

primary oscillation: $Re_D(\dfrac{\delta^*}{D})^{1/2} = \dfrac{u}{\nu}(\delta^* \cdot D)^{1/2} \geq \mathbf{800}$

secondary oscillation: $Re_{\delta^*} = \dfrac{\delta^* \cdot u}{\nu} \geq \mathbf{150}$

with δ^* : displacement thickness of the undisturbed boundary flow [m]
          D   : diameter of the pile [m]
          u   : free-stream velocity [m/s]
          υ : viscosity of the fluid [-]

Under waves no horseshoe vortices occur when the Keulegan-Carpenter number KC < O(6). This boundary varies depending on the Reynolds number.
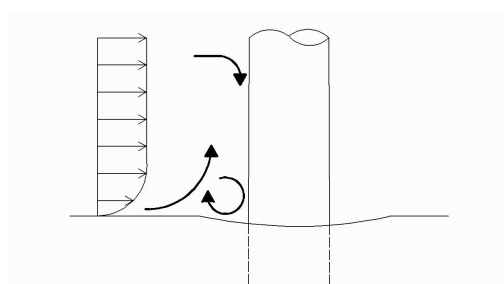
Figure 2-4: Formation of Horseshoe-vortices

Diffraction and reflection: Waves impinging on an obstacle reflect and bend around it. Only large piles change the wave field considerable. Diffraction and reflection are valuated as significant for D/L > 0.1 by Verheij and Hoffmans (1997) and by the Coastal Engineering Manual (2003) and for D/L > 0.2 by Sumer and Fredsoe (2002) and Hoffmans and Verheij (1997).

Figure 2-5 shows a typical wave field around a large circular pile.
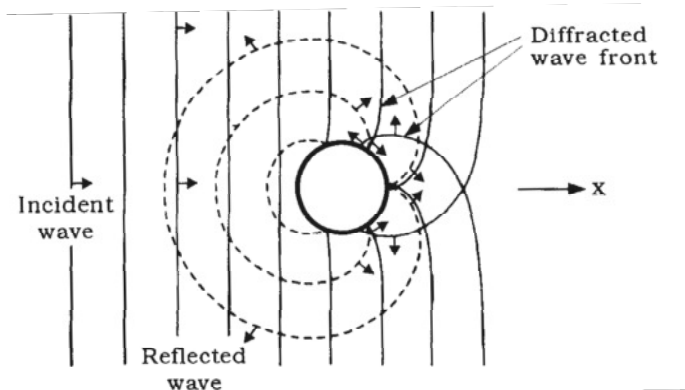
Figure 2-5: Diffracted wave field around a circular pile [Sumer and Fredsøe, 2002]

2.1.2   Definition of flow regimes:

Considering the described phenomena and the main drivers of scour the flow regimes are classified as follows:

KC > O(6)   : slender piles   or   slender-pile regime

KC < O(1)   : large piles   or   diffraction regime

O(1) < KC < O(6): intermediate piles   or   intermediate regime
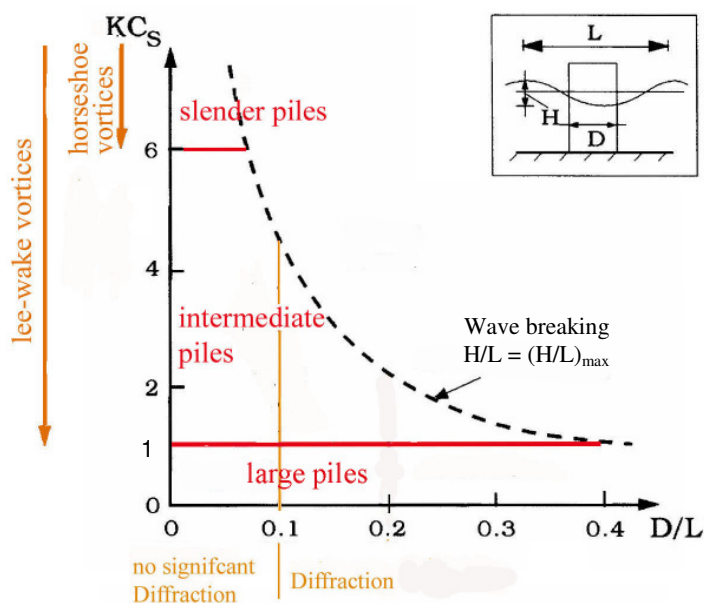
Figure 2-6: Demonstration of the flow regimes according to KC and D/L (based on Sumer and Fredsøe, 2002)

The categories of flow regimes are visualised in Figure 2-6. In Figure 2-7, 2-8 and 2-9 the flow characteristics according to slender and large piles are illustrated. Boundaries for the current only situation are not defined, this case does not play a role offshore and by interaction of wave and current the defined boundaries can be applied.
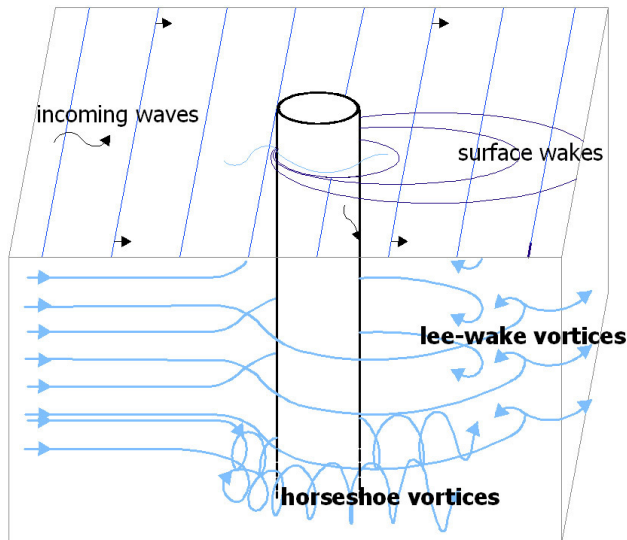
Figure 2-8: Illustration of the flow regime around slender piles
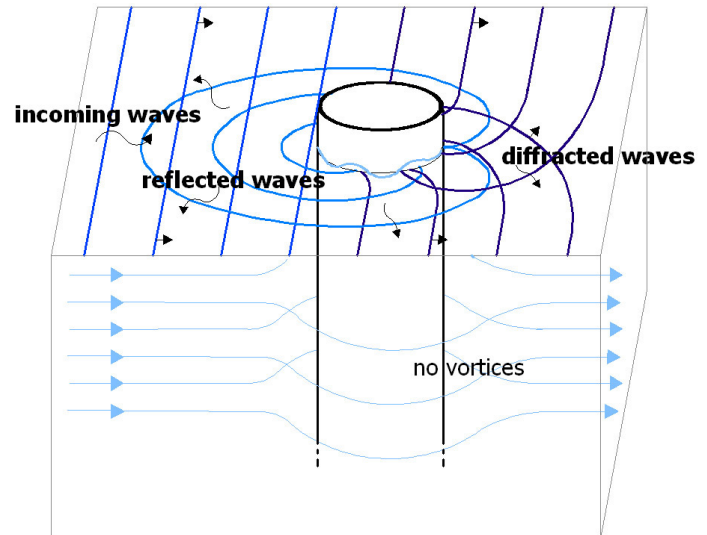
Figure 2-7: Illustration of the flow regime around large piles
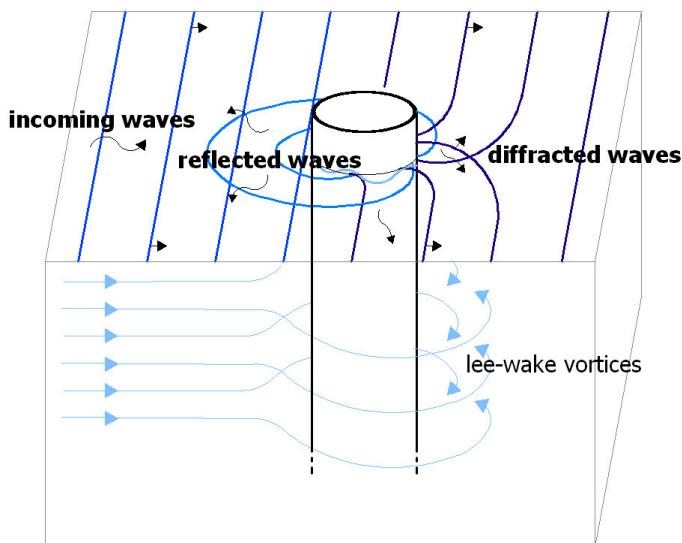
Figure 2-9: Illustration of the intermediate flow regime

In literature the regimes are sometimes defined differently. The definitions of flow regimes correspond principally to those from Sumer and Fredsøe (2002). The only difference is that Sumer and Fredsøe define the diffraction to be significant for $D/_L > 0.2$. Since other researchers (Verheij and Hoffmans, 1997; Coastal Engineering Manual, 2003) believe diffraction to be significant already for $D/_L > 0.1$, this boundary was chosen as basis of this thesis. Whitehouse (1998) defines slender piles over the water depth h as h/D > 2 and piles showing a ratio of diameter to wave length larger than 0.2 are dominated by the wave regime. As can be seen in Figure 2-7 this fits quite well to the defined regimes. Saito et al. (1990), who investigated extensively scour at large piles, defined slender piles with KC > O(5) and $D/_L < 0.2$ and large piles as KC < O(4) and $D/_L > 0.2$. This will be discussed in Section 4.2.3.

A classification of foundation piles of offshore wind turbines is given in Chapter 5. Slender piles are characterised by the vortices and described in Chapter 3. The flow and scour processes around large piles are not fully understood. Chapter 4 provides information about the current level of knowledge. In Chapter 5 and 6 this is analysed and it is discussed whether the order of the maximal scour depth in this flow regime can be evaluated.

In the intermediate flow regime the scour process is mostly determined by diffraction. However, the influence of the lee-wake vortices may not be neglected. The understanding of this flow regime is very limited. The standard of knowledge is summarized in Chapter 4, the predictability of scouring in this regime is discussed in Section 5.2.

2.1.3   Breaking waves:

Another phenomenon, which is of interest in this research, is the occurrence of breaking waves, since breaking waves can immensely increase the scour potential around a structure: Waves break when a maximal steepness $(H/L)_{max}$ is exceeded. The breaking criterion depends on the form of the orbital motion. Under deep-water conditions ($h/L \geq 0.5$) and in an intermediate water depth ($0.5 \geq d/L \geq 0.05$) the maximal wave steepness is identified as

$$(H/L)_{max} = {}^1/_7 \cdot \tanh (kh) \qquad\qquad (2.1)$$

 (Miche, 1951)

with   H : wave height [m]
          L : wave length [m]
          $k = 2 \pi/L$ (wave number) [-]
          h : water depth [m]

For random sea states the breaking condition is approximated to be at

$$(H/h)_{max} = 0.6 \text{ to } 1.2 \qquad\qquad (2.2)$$

(according to Oumeraci, 1996)

2.2 Morphodynamic and morphological Processes

This section deals with loose, non-cohesive sand grains. Structures at cohesive sea-beds are less at risk of scour, because the cohesive forces slow down the scour process. Non-cohesive sea-beds are widely spread and common in model tests.

In the first sub-section, the focus is on a single grain. By determining the forces acting on the grain the initiation of motion is valuated. In the second sub-section, the evaluation of scour by the bed shear stress is introduced.

For the development of scour, a flow away from the structure must exist and the conditions upstream need to be considered. This is explained in more detail in Subsection 2.2.3 by defining live-bed and clear-water scour.

2.2.1 Forces acting on a sand grain

The initiation of movement can be described over the equilibrium of forces. Therefore, the forces acting on a single sand grain are explained and quantified in the following paragraphs, afterward the equilibrium is drawn up.

Forces which hold the grain in place are called resistant forces. The only resistant force in the static analysis is the gravity force. Forces leading to the movement of the grain are called mobilising forces. The mobilising forces are the drag force, the lift force and the inertia force of the water particles.

Gravity Force:

For the gravity force of a sand grain on the bottom of the sea the submerged weight need to be considered. The submerged weight is equivalent to its volume times the density of the sediment minus the density of the surrounding water. Therewith the gravity force is defined as follows:
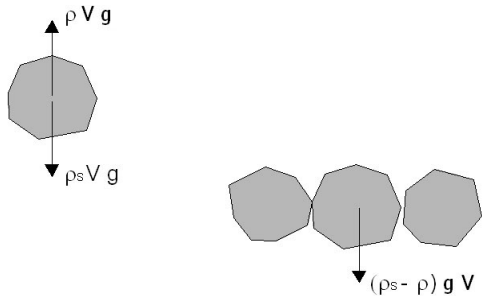
$$F_G = (\rho_s - \rho)gV \qquad (2.3)$$

with
F_g : gravity force $\quad$ [N]
ρ_s : density of the grain $\quad$ [kg/m^3]
ρ : density of water $\quad$ [kg/m^3]
g : acceleration of gravity $\quad$ [m/s^2]
V : volume of the grain $\quad$ [m^2]

Figure 2-10: Illustration of the gravity force

Drag Force:

Through sub-pressure behind the grain and viscous skin friction a force in the direction of the flow is acting on the grain. This force is called drag force and defined as

Figure 2-11: Illustration of the drag force
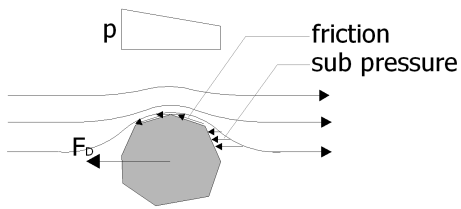
$$F_D = \frac{1}{2} C_D \rho u_b^2 A_D$$

(2.4)

with F_D : drag force   [N]
       C_D : drag coefficient   [-]
       ρ : density of water   [kg/m³]
       u   : velocity of the flow near the bottom   [m/s]
       A_D : exposed surface area   [m²]

Lift Force:

The lift force is caused by lower pressure at top of the grain through contraction of the water streamlines along the sides. The drag force acts perpendicular to the drag force and can be evaluated as

Figure 2-12: Illustration of the lift force
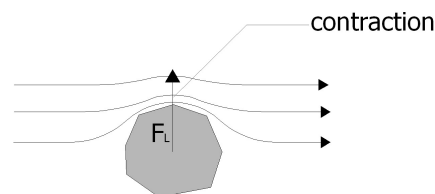
$$F_L = \frac{1}{2} C_L \rho u_b^2 A_L$$

(2.5)

with F_L : lift force   [N]
       C_L : lift coefficient   [-]
       ρ : density of water   [kg/m³]
       u   : velocity of the flow near the bottom   [m/s]
       A_L : exposed surface area   [-]

Inertia force:

According to Newtons second law, accelerated masses possess an inertia force. Hence, accelerated water particles impinging on a sand grain apply an acting force out of their acceleration. Following Newton the order of this force is the product of the mass of the water particles times their acceleration. Following the Morrison equation (1950), which is given in Eq. (2.6) the form of the sand grain can be evaluated.

$$F = F_D + F_i = \frac{1}{2} C_D \rho_A u_b |u_b| + C_M \rho_V \frac{Du}{Dv}$$

(2.6)

Morrison (1950)

with   F   :   force on an object   [N/m²]
        F_D :   drag force   [N/m²]
        Fi   :   inertia force   [N/m²]
        C_D :   drag coefficient   [-]
        C_M :   shape coefficient   [-]
        ρ :   density of water   [kg/m³]

The shape coefficient depends on the shape of the cross section. For coarse sediment Terrile(2004) suggest C_M to be between 2 and 3.

Initiation of Motion:

The grain moves if the moment of forces around the point of contact with the adjacent grain is positive: Kirchner (1990) (according to Tromp, 2004) determined that the easiest movement is under β = 30-45° (angle of initiation of movement or pivoting angle).
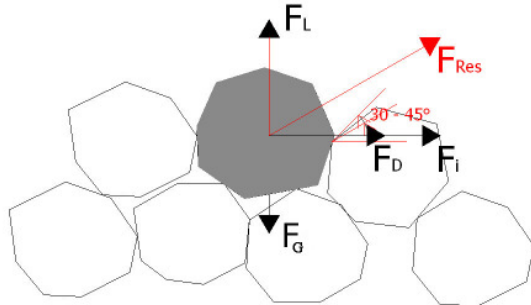
Figure 2-13: Illustration of the equilibrium of forces

By formation of the equilibrium of forces the initiation of motion is determined as

$$F_G sin\beta < (F_i + F_D)cos\beta + F_L sin\beta \qquad (2.7)$$

with $30° < \beta < 45°$ (pivoting angle)

2.2.2 Bed shear stress

The most common approach to describe the initiation of movement is by using the Shields parameter.
Shields (1936) recognized that the initiation of motion can be described by the ratio of the critical shear stress to the normal stress. This quotient is known as the critical Shields parameter ψ_c and was empirically evaluated as a function of the particle Reynolds number Re*:

$$\Psi_C = \frac{\tau_C}{(\rho_s - \rho_w)gd} = \frac{u_{*c}^2}{\Delta gd} = f(Re_*) \qquad (2.8)$$

with ψ_c : Shields parameter   [-]
      τ_c : critical shear stress   [N/m^2]
      u_{*c} : critical shear velocity   [m/s]
      ρ_s : density of stone   [kg/m^3]
      ρ_w : density of water/fluid   [kg/m^3]
      g   : gravitational acceleration   [m/s^2]
      Δ : relative density (ρ_s - ρ_w) / ρ_w [-]
      Re$_*$: particle Reynolds number ^   [-] (see appendix A)

The denominator can be understood as gravity force related to the area of a grain. This is illustrated in Figure 2-14.
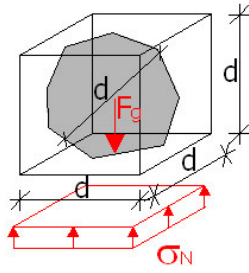
$$\sigma_N = \frac{F_g}{d^2} = \frac{(\rho_s - \rho_w)gV}{d^2} \approx \frac{(\rho_s - \rho_w)gd^3}{d^2}$$

$$= (\rho_s - \rho_w)gd \tag{2.9}$$

Figure 2-14: Illustration of the normal stress

The numerator can be deduced in the same way from the summation of drag force and lift force:

$$\left. \begin{aligned} \frac{F_L}{A_L} &= \frac{1}{2}C_L\rho u^2 \\ \frac{F_D}{A_D} &= \frac{1}{2}C_D\rho u^2 \end{aligned} \right\} \quad \tau_c = C_D\rho u^2 \tag{2.10}$$

For circular shapes like sand grains the drag coefficient $C_D \cong 1$. The new drag coefficient is the sum of lift and drag coefficient divided by 2.

In the case of cyclic loading like under waves the bed shear stress should be evaluated by the wave friction coefficient:

$$\tau_w = \frac{1}{2}f_w\rho u^2 \tag{2.11}$$

(Swart, 1976)

with $\quad f_w = exp[-5.977 + 5.21(\frac{k_s}{a})^{-0.194}] \quad$ if $\quad \frac{k_s}{a} > 1.47$

$\quad\quad f_w = 0.32 \quad\quad\quad\quad\quad\quad\quad\quad\quad$ if $\quad \frac{k_s}{a} \leq 1.47$

τ_w	:	shear stress due to waves	[N/m^2]
f_w	:	wave friction coefficient	[-]
ρ	:	density of water	[kg/m^3]
u_m	:	maximal orbital velocity	[m/s]
k_s/a	:	relative roughness height	[-]
a	:	amplitude of the orbital motion	[m]
k_s	:	bed roughness length	[m]

with different definitions of k_s:
$k_s = 2.5\ d_{50}$ (Nielson 1992)
$k_s = 3\ d_{50}$ (Van Rijn, 1993)

The comparison of the derivation of the Shields parameter with the forces acting on a grain (Section 2.2.1) shows, that the inertia force is not taken into account in the evaluation by Shields. This needs to be considered by the evaluation of sediment transportation in an accelerated flow. The influence of the inertia force of the water particles on sediment transport was recently investigated by Terrile (2004), Tromp (2004), Dessens (2004).

For the sediment motion in a steady current the dependence of the Shields parameter to the particle Reynolds number was evaluated by Shields himself. Figure 2-15 shows the original Shields curve (dashed line) and its modification by Sleath (1978). The Sleath curve is related to sediment motion under waves and therewith a better basis for the scour process around offshore wind turbines. The initiation of motion is indicated as a grey area, because the initiation of motion can be understood as the rolling of a single sand grain up to the motion of all grains. Values below the curves indicate no motion.
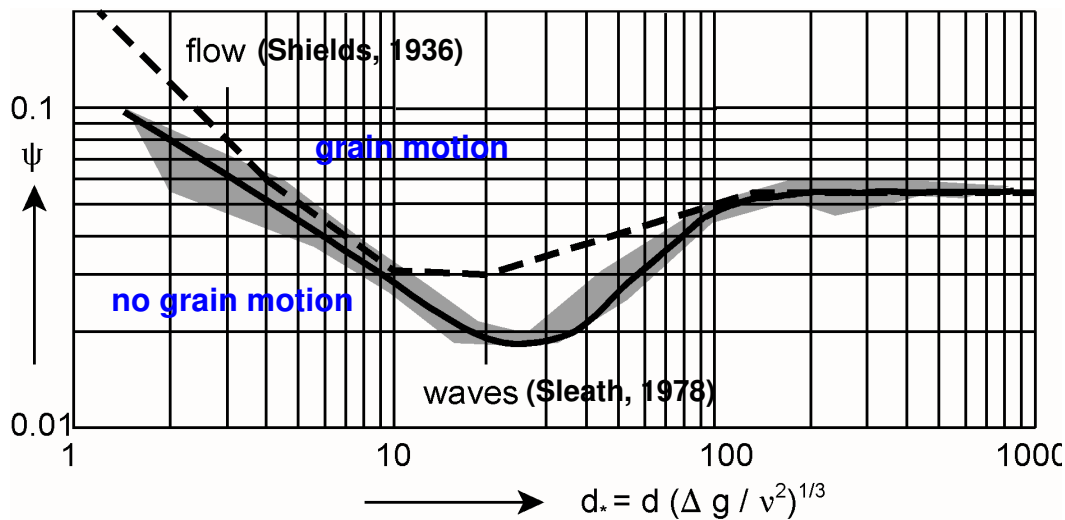
Figure 2-15:   Shields (for current) and modified Shields curve (for waves) (Sleath, 1978 according   to Terrile, 2004)

2.2.3   Equilibrium scour depth

Scour develops until the sediment transport potential in the undisturbed flow is as high as the sediment transport potential at the pile. This leads to a maximal possible scour depth, the so-called equilibrium scour depth. That means, that not only the state in the vicinity of the structure (area of disturbed flow) needs to be known, but also the state in the undisturbed area upstream of the structure.

Whether sediment is in motion in the undisturbed area or not, the scour process is defined as clear-water scour or live-bed scour:

Clear-water scour:

undisturbed area: $\tau_0 < \tau_c$
vicinity of structure: $\tau_0 \cdot M > \tau_c$

with τ_0 : ambient bed shear stress   [N/m^2]
         τ_c : critical value for sediment motion   [N/m^2]
         M : shear stress amplification factor due to the presence of the structure [-]

Under these conditions there is only sediment motion in the vicinity of the pile. The scour equilibrium is reached, when the equilibrium of forces (reference to earlier Eq. 2.7) is balanced again or $\tau_0 \cdot M = \tau_c$.

Live-bed scour:

undisturbed area: $\tau_0 > \tau_c$

vicinity of structure: $\tau_0 \cdot M > \tau_c$

Under these conditions, also the undisturbed bed is subject to sediment motion. Through the amplification factor the sediment transport potential near the pile is higher than upstream of the pile. As a result scour develops at the pile.

The equilibrium scour depth is reached when the sediment transportation potential, which can be evaluated over the bottom shear stress, at the pile is as large as in the undisturbed area:

$$\tau_0 \cdot M = \tau_c \qquad\qquad \text{with } M = 1.0$$

2.2.4   Transport rate

Scour can not be evaluated only by determining whether sediment is in motion or not. The formation of local erosion requires that the sediment transport potential of the fluid is higher than the upstream sediment transportation rate. In Eq. (2.12) the basic sediment equation for the 2-dimensional case is shown.

$$\frac{\partial \zeta}{\partial t} = -\frac{1}{1-\varepsilon}\Big[\frac{\partial q_s}{\partial x} + \frac{\partial q_s}{\partial y} + \nabla_D(x,y) - \nabla_E(x,y)\Big] \qquad (2.12)$$

(Whitehouse, 1998)

with
	ζ	: elevation of the seabed	[m]
	$\partial \zeta/\partial t$	: changing of elevation over time	[m/s]
	ε	: bed porosity (converts volume flux of sediment to volume of material including pores)	[-]
	q_s	: sediment transport rate	[m^3/s]
	$\partial q_s/\partial x$	: flux of sediment passing through a unit of length	[m^3/ms]
	∇_D	: sediment deposition	[m^3/ms]
	∇_E	: sediment entrainment	[m^3/ms]

Under consideration of the void ratio and the initiation of motion the volumetric net sand transport rate q can be determined by

$$\vec{q} = A(\psi_m - \psi_c)(\vec{u_m} + \alpha\vec{u_c})d_{50}\frac{1}{1-\lambda_\nu} \qquad (2.13)$$

(Saito et al., 1990)

with
	q	: volumetric net sand transport rate	[m^3 s/m]
	A, α	: non-dimensional coefficients	[-]
	ψ_m	: momentary Shields parameter	[-]
	ψ_c	: critical Shields parameter	[-]
	u_m	: steady drift velocity of waves	[m/s]
	u_c	: depth-integrated velocity of the current	[m/s]
	d_{50}	: averaged diameter of sand particle	[m]
	λ_v	: void ratio of sediment	[-]

The afore mentioned approach is simplified. It bases on Whitehouse (1998) and Saito et al. (1990). A more complex evaluation can be found in Zhao et al. (2004). To model scour deposition or entrainment is evaluated in finite elements, differences or volumes. This requires a considerable effort on calculation and programming which exceeds the scope of this thesis.

The consideration of the transport rate enables to determine the equilibrium scour depth under live-bed conditions, which is smaller and more common than clear water scour. It is also an important method to determine the time scale of scour. The time scale is especially important to predict the maximal scour process in tidal currents or during construction.

2.2.5   Liquefaction

Another morphodynamic phenomenon which needs to be considered in the design of an offshore wind turbine is the liquefaction of the sea bed. Liquefaction appears when the volume is reduced faster than the pore water can discharge. The effective stress between the grains is vanished. The water-sediment mixture behaves like a fluid. Since this means not only the structure, but also the scour protection would fail, liquefaction is not considered in this research. In the design liquefaction needs to be analysed separately. Readers are recommended to take notice of the work of Sumer and Fredsøe (2002) and the proceedings of LIMAS, a liquefaction research project of the European Union (2004).

2.3   Effect of Scour on Foundation Stability

Figure 2-16 shows a sketch of an offshore wind turbine with common dimensions. The design scour depth of 1 to 1.5 times the diameter (Det Norske Veritas (DNV), 2004) equals about 20 to 25% of the foundation depth.

Scour: for $^S/_D$ = 1.0 - 1.5
        the design scour depth is
        4 to 6 meter
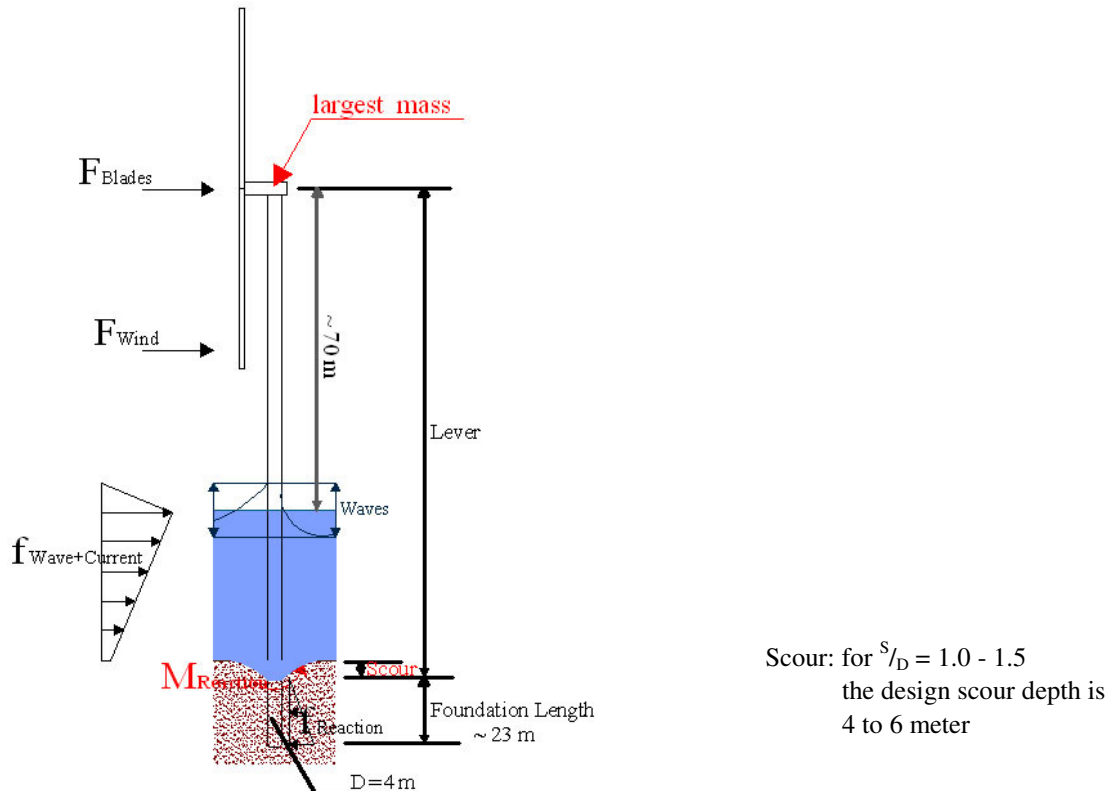
Figure 2-16: Sketch of a monopile-founded wind turbine (including example dimensions
determined for a wind turbine in 25 meter deep water in the Themse estuary)

Designing an offshore wind turbine three basic proofs need to be verified:

- The maximal moment need to be sustained by the monopile and transferred into the ground over the foundation length. (static analysis)
- To avoid resonance, the natural frequency of the structure must not correspond with the natural frequency of the loading waves. (dynamic analysis)
- The pile need to resist all load cycles over its lifetime. (fatigue analysis)

The basics of these proofs and the effects of a scour hole are described in the following sections.

2.3.1   Static Analysis

In the static analysis the stability of the turbine under extreme conditions is proofed. For offshore wind turbines the survival conditions are normally related to the once in 100-years design event. Not always is the maximal loading caused by the survival conditions. During storms the blades do not produce power. Under operation the horizontal loading on the blades is much higher and by the long lever this can also lead to the maximal design moment as well.

It is obvious that the foundation length is decreased through a scour hole. In the same manner the lever of the horizontal loads increases. Therewith a scour hole leads to the decrease of the foundation length and an increase of the maximal moment.

The static analysis is rarely design driving.

2.3.2   Dynamic Analysis

In the dynamic analysis it must be verified, that the natural frequency of the structure remains from the frequency of the loading waves. The correspondence of the natural frequency with the loading frequency means resonance. Resonance would lead to an immense increase of the amplitude of the deformation of the structure and its foundation.

The nacelle (~ 60 t) forms most of the mass of the complete structure (~ 140 t). For statements concerning the dynamic analysis it is adequate to simplify the system to a single mass system. This is shown in Figure 2-17. For the simplified system the frequency can be determined by the Reynolds method. The required formula is given in Eq. (2.11) (Zaaijer, 2004b).

$$f_1 = \frac{D}{l^2} \sqrt{\frac{E}{104(\frac{m_{top}}{\pi D t l} + 0.227\rho)}} \tag{2.14}$$

with f_1 : natural frequency $[^1/_s]$
   D : diameter of the pile   [m]
   l : lever   [m]
   E : modulus of elasticity $[N/m^2]$
   m_{top} : mass at the top   [kg]
   t : thickness of the wall [m]
   ρ : density of the pile $[kg/m^3]$

Figure 2-17: Wind turbines simplified to a single mass system (Zaaijer, 2004b)

By the formation of a scour hole the lever increases and therewith the natural frequency of the structure decreases.

Tempel et al. (2004) analysed the influence of a scour hole on the natural frequency. They determined the natural frequency for three different pile designs. Their result is displayed in Figure 2-18. The red box marks the area of the design rules of Det Norske Veritas (DNV) which are mostly used by designing an offshore wind turbine.
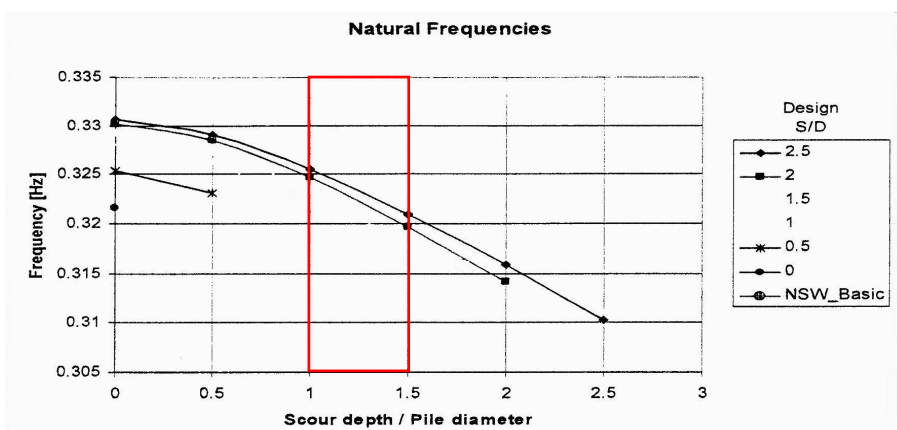
Figure 2-18: Effect of scour depth on natural frequency of monopile structures (Tempel et al., 2004)

In Figure 2-19 the range of wave frequencies and natural frequency are shown.
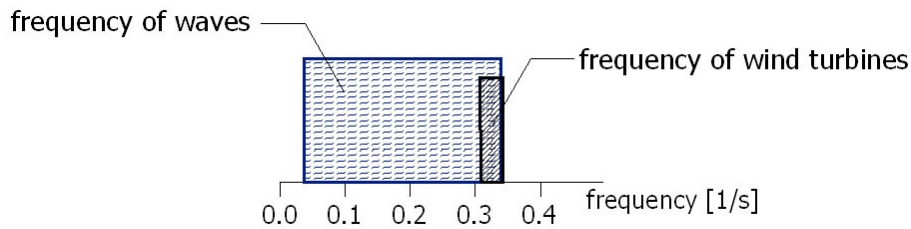
Figure 2-19: Confrontation of wave frequencies and natural frequencies of wind turbines

The natural frequency of the wind turbine overlaps for a greater part with the wave frequency. The loading wave field consists of a spectrum of frequencies and the high frequency waves have less energy.

Tempel et al. (2004) concluded that the impact of the scour depth on the natural frequency is minor.

2.3.3   Fatigue Analysis

The pile does not only need to resist the maximal moment, but also the load cycles through its lifetime. The lifetime is normally set to 20 years. The fatigue analysis adverse the load cycles expected during the life-time of the structure and its stress amplitudes.

This is done by building up a stress histogram as illustrated in Figure 2-20. For every stress amplitude the number of expected load cycles is evaluated of a stress history. The stress history is based on scatter diagrams for wind and wave loading and a steady loading by current. An example of a scatter diagram is given later in Table 5-4. Beside the expected loading also the number of load cycles which the structure can resist for each stress amplitude, is charted in the stress histogram. Therefore the crack propagation and the occurrence of plastic deformations are evaluated. By the fatigue analysis it must be shown that the graph which indicated the failure of the structure is not overlapping with the expected stress cycles.
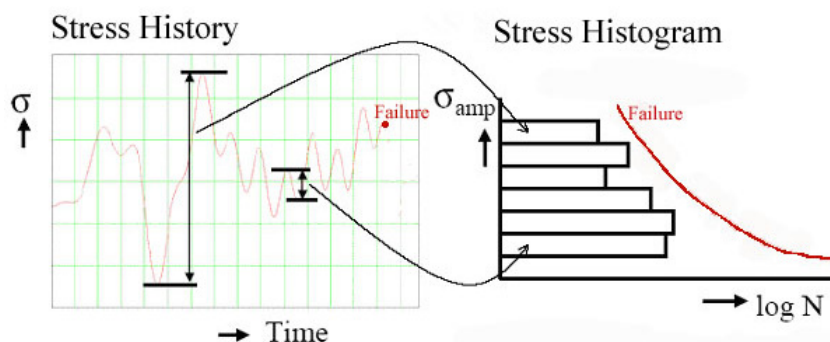
Figure 2-20: Evaluation of the fatigue resistance (Zaaijer, 2004)

The fatigue analysis often represents the main focus in the design of a monopile-founded wind turbine.

In the previous subsections it was explained, that the moment increases and the frequency decreases by the formation of a scour hole. For the fatigue analysis this means higher stress

ranges and more load cycles. Both effects have a negative impact on the fatigue behaviour. Tempel et al. (2004) analysed the impact of a scour hole on the fatigue analyses as well. The result is displayed in Figure 2-21. The red box marks the design scour depth by the DNV. At the vertical axis the fatigue damage D_{life} is illustrated. A fatigue damage of 1.0 indicates a fatigue life time of 20 years. In the design a fatigue damage of less than 0.33 is aimed for.
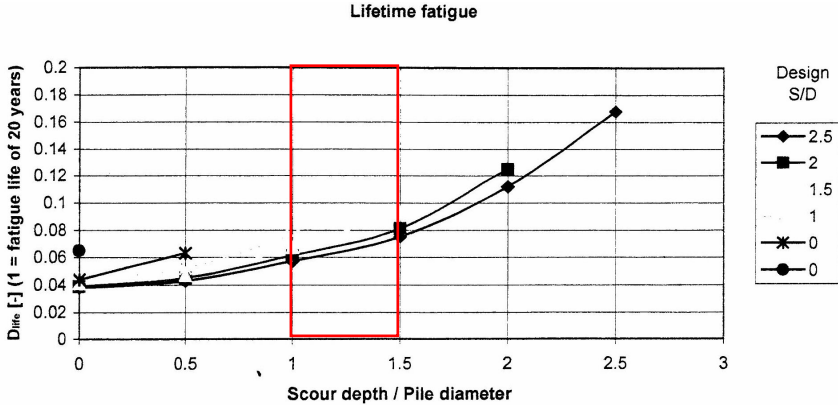
Figure 2-21: Effect of scour depth on fatigue lifetime of monopile structure (Tempel et al., 2004)

Even though the proofed designs were chosen far from the design limits (D_{life} < 0.33), the increase of the fatigue life in dependence of the scour depth is strong. Therewith the conclusion of Tempel et al. (2004) was that the fatigue analysis is sensitive to the scour depth.

3   Scour around Slender Piles

Piles are called slender if

$$KC > 6$$
$$^D/_L < 0.1$$

As described in Chapter 2 scour in this regime is mainly generated by lee-wake and Horseshoe vortices. These are illustrated in Figure 2-7. A minor role in the scour process plays the local acceleration due to the contraction of the flow. The incident waves are not significantly affected by the pile.

Scouring around slender piles has been widely investigated, because the slender-pile regime dominates in practice. However a fully theoretical or numerical description of flow and the sediment transport does not exist.

Since good references summarising the state of knowledge exist (the author recommends Whitehouse (1998), Sumer and Fredsøe (2002), Unruh and Zielke(2004), this thesis focuses on scouring at large piles, the processes are not explained in detail nor are all established formulas introduced. In the following section important formulas and characteristics for the discussions in Chapter 5 and 6 are summarized.

3.1   Equilibrium scour depth

The scour depth under waves was recognized to be mainly dependent on the Keulegan-Carpenter number (see Appendix A) and the diameter of the pile. The most common equation to determine the equilibrium scour depth was set up by Sumer et al. (1992) (acc. to Whitehouse (1998), Sumer and Fredsøe (2002), Hoffmans and Verheij (1997), Sumer et al. (2001a)). This formula is given in Eq. 3.1 and illustrated in Figure 3-1. In conformance with the regime definition this formula is valid for KC > 6. Further live bed conditions and regular waves are assumed.

$$\frac{S}{D} = 1.3 \left[1 - exp(-m(KC - 6)) \right]$$
$$= 1.3 \left[1 - exp(-m(\frac{U_m T}{D} - 6)) \right] \tag{3.1}$$

with   m = 0.03 for regular waves
        m = 0.06 for non-linear waves[1]
        S   : equilibrium scour depth
        D   : pile diameter
        KC   : Keulegan–Carpenter number
        U_m : maximal undisturbed orbital velocity at the bed
        T   : wave period

The illustration points out that the scour depth is maximal under steady currents (KC → ∝) where the scour depth reaches a value of 1.3 times the pile diameter. Aside from the illustration of Eq. 3.1 Figure 3-1 shows how 53 experimental results fit the estimation.

Another common rule had been introduced by Breusers et al.(1977): The maximal design scour depth is recommended as 1.5 times the pile diameter. This is a simplification of scour formula of Breusers et al. (1977).

---

[1] Waves are non-linear if the Ursell number $U = HL^2/h^3 > O(1)$.

The relation between the scour depth and the pile diameter following Breusers rules and those from Sumer and Fredsøe are shown in Figure 1-2.
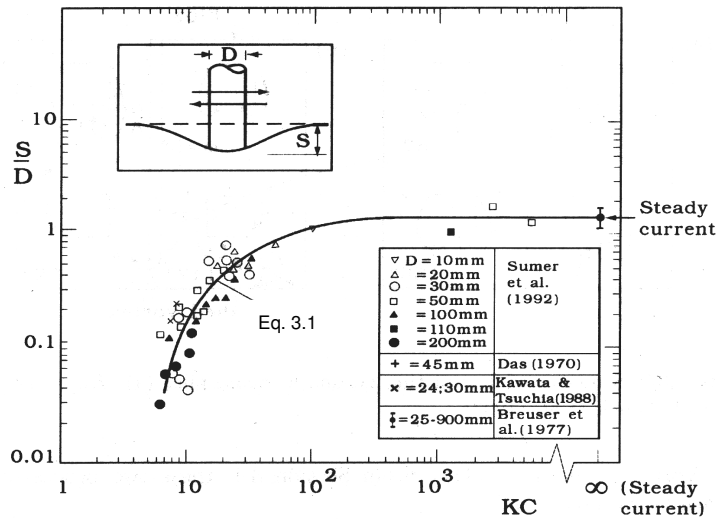
Figure 3-1: Equilibrium scour depth for slender piles (KC > 6) under live bed conditions and regular waves (Sumer et al., 1992)

Under the combination of waves and current the scour does not represent a linear superposition of both effects. The maximal scour depth can be evaluated by the velocity ratio as defined in Eq. (3.2) and shown in Figure 3-2.

$$U_{cw} = \frac{U_c}{U_c + U_m} \tag{3.2}$$

(among others: Sumer and Fredsøe (2002))

with U_{cw} : velocity ratio of current velocity and maximal undisturbed orbital velocity
       U_c : current velocity
       U_m : maximal undisturbed orbital velocity at the bed

Eq. (3.2) is valid for velocity ratios up to $U_{cw} > 0.7$, for a higher U_{cw} the scour depth is equivalent to the current only case.
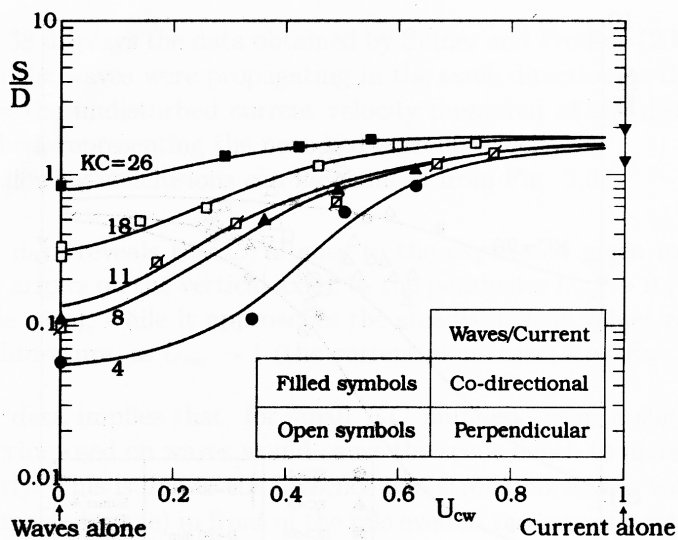
Figure 3-2: Interaction of waves and current (Sumer and Fredsøe, 2001a)

The maximal scour depth in the current only case can be predicted best by the CSU (Colorado State University) equation. Since the current only case is not relevant at the sizes of wind turbines it is referred to the Scour Engineering Manual and Hoffmans and Verheij (1997).

3.2   Time development

Sumer et al. (1992a) and Fredsøe et. al. (1992) [according to Whitehouse] derived the most acknowledged formula of the determination of the time scale (Whitehouse, Sumer and Fredsøe 2002) as follows:

$$T_S = \frac{D^2}{[g(\frac{\rho_s}{\rho} - 1)d_{50}^3]^{1/2}} T^*$$

(3.3)

$T^* = 10^{-6}(\frac{KC}{\theta})^3$ for waves

$T^* = \frac{1}{2000} \frac{\delta}{D} \theta^{-2.2}$ in steady current

with | T_s | : | characteristic time-scale for scour
| T^* | : | dimensionless time-scale for scour
| D | : | pile diameter
| g | : | gravity acceleration
| ρ_s | : | density of the sediment
| ρ | : | density of water
| d_{50} | : | median diameter of the sand grains
| KC | : | Keulegan Capenter number
| Θ | : | Shields parameter
| δ | : | thickness of the boundary layer

3.3   Scoured area

The equilibrium scour hole around a slender pile forms an ellipse. In a steady stream the length of the scour hole behind the pile is up to 5 times the diameter (Whitehouse, 1998). Therefore Whitehouse recommends the scour protection to be installed over a radius of up to 5 times of the pile diameter. Sumer and Fredsøe (2002) recommend the radius of the scour protection referring to Melville and Coleman (2000) as 2 times the diameter.

Because of the high uncertainties the diameter of the scour protection area extends up to 7 times of the pile diameter as best practice (Halfschepel, 2001; Zaaijer, 2004).

3.4   Influences of breaking waves

Under breaking waves the orbital velocity of the water particles highly increases. Therewith the scour under breaking waves is much larger than under normal waves.

Bijker and de Bruyn (1988) recognized that the experimental modelling of scouring due to breaking waves is not effective. They believed the reason is the impossibility of adequate modelling of the bed roughness. The sand grains can not be decreased by the same scale as the rest model, since this would lead to cohesion. So the roughness of the sea bed in model experiments is larger than in nature. Experimental modelling of scour under breaking waves leads to smaller scour depth than detected in nature.

Only limited measurements of scour depth under breaking waves are available. The scour depth to pile diameter ratio S/D reaches values up to 3 (Bijker, 1988).

4   Scour around Large Piles

As defined in Chapter 2 the notation "large" pile refers to pile-wave-conditions with a Keulegan-Carpenter number **KC < O(1)**. Under this condition the flow is dominated by diffraction and reflection. For **KC < O(1)** no vortices are formed.

This chapter deals also with scouring around intermediate piles. The intermediate regime includes piles with **O(1) < KC < O(6)**. Equal to large piles the flow regime is dominated by diffraction and reflection. Besides lee-wake vortices appear and influence the flow.

These flow regimes and scour processes are not understood in every detail, nor do generally accepted formulas for the scour depth exist. Table 4.1 gives a review of the most important steps of research. Nearly no experiences are available of the intermediate flow regime.

Table 4.1: History of research at large piles

History:
1980: **Rance** did first researches about the scour regime at large piles resulting in a maximal scour depth of 4% of the pile diameter.
1985: **Toue and Katui** did first experimental investigation of the sediment movement around a large circular cylinder.
1990: **Saito, Sato and Shibayama** presented first attempt of a numerical model for the changes of the bottom topography. Progressed by the finite differences method and dividing the process into a wave model, a current model and a sand transport model.
1992: **Katsui and Toue** improved their model by using the wave-current friction factor and examined its influence as mean current on sediment transport
1992: **Saito and Shibayama** improved their model by considering a uniform bottom slope and steady currents
1997: **Sumer and Fredsoe** performed detailed velocity measurements in the vicinity of a large pile exposed to regular waves and discovered the cycle-to-cycle variation
2001: **Sumer and Fredsoe** examined the steady-streaming flow of scour process around large vertical circular cylinders, in particular the influences of KC and D/L
2004: **Zhao, Teng** and **Li** presented a different approach of a numerical model for wave-current action using the finite element method, waves simulated by hyperbolic mild-slope equation, currents by shallow-water equation and integration over the depth. The sediment transportation rate is evaluated by the summation of the shear stress induced by waves and currents and a diffusion equation.

In this chapter the state of knowledge is reviewed and analysed. This is done in three parts. Section 4.1 deals with the flow and scour characteristics. In Section 4.2 the scouring is analysed empirical. In Section 4.3 theoretical models of the flow regime are presented and evaluated. A summary of this chapter is given in Section 5.1. To understand the steps of the analyses it is referred to the overall illustration of the approach in Figure 5-1.

4.1   Scour processes

In this section the topography of the scour hole, the diffracted wave field around circular piles and the wave induced flow are reviewed.

Researchers of scour around large piles agree, that the impact by waves and current can be analysed independently (Whitehouse, 1998; Toue et al., 1992; Zhao et al., 2004). Their combined influence on the sediment transportation is evaluated best by the summation of the induced bed shear stresses (Zhao et al., 2004; Nielson and Callaghan, 2002). The current induced flow around a cylinder is not explained in this section, since it follows the principle of basic hydrodynamics. It is explained in Section 4.3.2.

4.1.1   Topography of the scour hole

The scour hole around large piles is basically different than around slender piles: In the vicinity of the pile not only scour, but also accumulation is formed. This can be seen in Figure 4.1, which shows a photo of the bed topography around a large pile. Scour occurs only on the rear side of the pile. At its front and lee accumulation areas are visible.
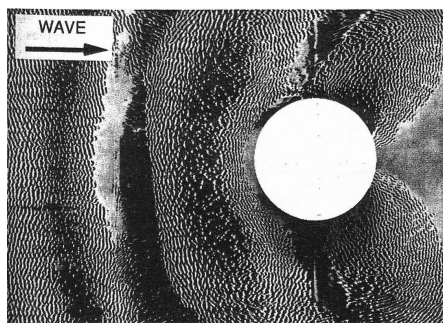
Figure 4-1: Photo of the bed topography around a large pile (Toue et al., 1992)
D = 117cm, T = 1.0s, H = 10cm, L = 1.37m, $^D/_L$ = 0.85, KC = 0.14, t = 2220s

In Figure 4-2 the topographies of scour holes measured by Sumer and Fredsøe (2001) under different wave conditions are shown. The area of scour and accumulation differs significantly. While in the experiment with KC = 1.1 scour is formed at the side and accumulation in the front and lee, the second experiment (KC = 0.61) results in accumulation at the sea side and scour at the lee and front.
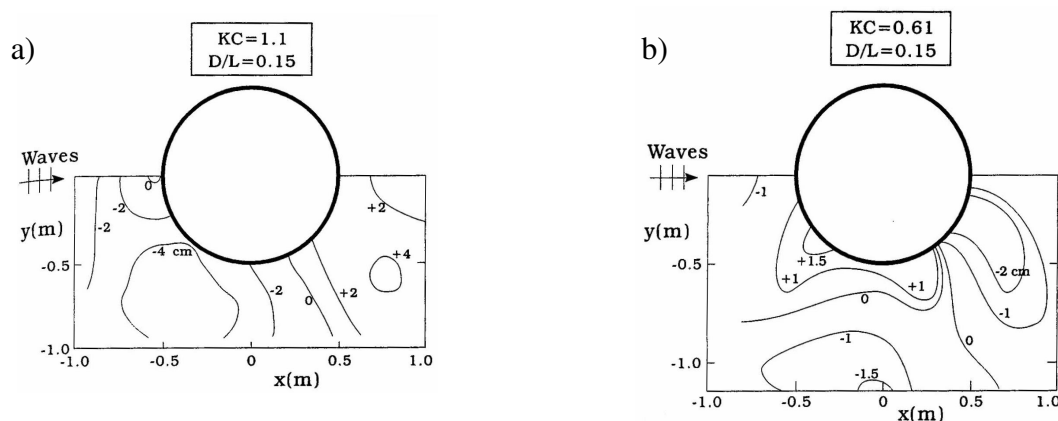
Figure 4-2: Contour plot of the bed topography of the equilibrium state at the same pile after different wave actions (Sumer and Fredsøe, 2001); D = 100 cm, T = 3.5 s, L = 6.8 m, $^D/_L$ = 0.15
a) H = 12 cm, KC = 1.1   b) H = 6.4 cm, KC = 0.61

No detailed investigations have been performed to understand the shape of the scour hole in dependence on the wave parameters. Sumer and Fredsoe (2001) published a short approach based on three experiments.

The author of this thesis believes in a close relation between the scour topography and the wave field. The scour topography as shown in Figure 4-1 has a similar shape as vortex ripples. Vortex ripples are formed under undisturbed waves as shown in Figure 4-3. On the left picture the orbital motion is directed to the right. The right picture shows the opposite. Under undisturbed waves they extend in lines parallel to the crests of the waves. The "sand ripples" in the vicinity of a large pile are parallel to the wave crests as well. This shows the comparison of Figure 4-1 and Figure 4-4. The latter shows a wave field measured around a large pile.
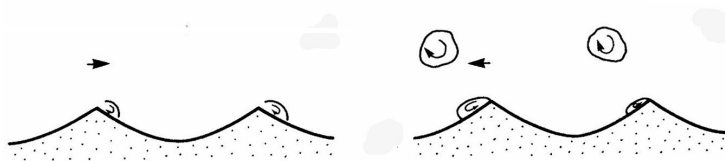
Figure 4-3: Sand ripples under short period waves (Fredsoe and Deigaard, 1992)

A second effect of the wave field on the bed topography is explained in Subsection 4.1.3.b. Due to the pressure distributions an upstream is formed under wave troughs and a downstream under wave crests. Sediment is transported by the stream, which means that sediment is transported from under the troughs (scour) to under the crests (accumulation).

4.1.2   The diffracted wave field

As described in Section 2.1 the wave field around a large pile is the superposition of incoming waves, reflected waves and diffracted waves. In Figure 4-4 the measured wave fields by Saito and Shibayama (1990) are shown. The left picture shows the wave field before scour took place. On the right the measured wave field in the equilibrium state is illustrated.

relative H = local H / incident H

■ > 1.4
■ 1.2 - 1.4
■ 1.0 - 1.2
■ 0.8 - 1.0
■ 0.6 - 0.8
■ < 0.6

a) before scour development   b) equilibrium state
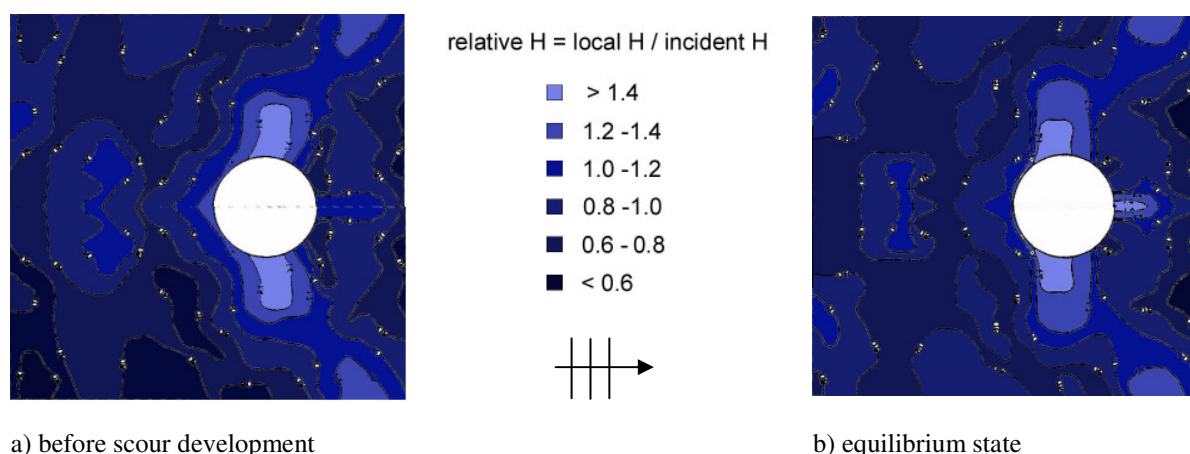
Figure 4-4: Wave field around a large pile as measured by Saito and Shibayama (1990)
        D = 52.2 cm, T = 0.94 s, H = h = 16.5 cm, L = 1.055 m, $^D/_L$ = 0.5

To understand the wave field it is helpful to have Figure 2-5 in mind, which shows the shapes of incoming, reflected and diffracted waves. The field of undisturbed incoming waves shows crests and troughs perpendicular to the wave propagation, which is shown in this thesis always from left to right. By the disturbance of the pile the crests and troughs, which are the superposition of incoming, reflected and diffracted waves, are bent around the pile. The wave amplitude increases more than 40%. In front of the pile the wave field is dominated by incoming and reflected waves and a standing wave is formed. The sheltered area in the back is dominated by diffracted waves.

The wave field changes little by the development of a scour hole. Differences are notable at the lee side of the pile.

In Subsection 4.1.1 it was already stated, that the shape of the wave field has a large impact on the shape of the scour hole. It was declared, that the scour topography is dependent on the ratio of the pile diameter with the wave motion, hence the Keulegan-Carpenter number KC. Because of the close relation between wave field and scour shape, also the wave field will change in dependence on KC. No measurements of the wave field were found to show this. It is unproved if further describing parameters like the diffraction factor $^D/_L$, hence pile diameter versus wave length, influence the shape of the wave field. It is most likely that the relation of pile diameter to wave length has an influence on the wave field. Also the scour extension, which is looked at in Subsection 4.2.2 b, is likely to depend on the ratio $^D/_L$.

4.1.3   Wave-induced flow

In the previous subsection and Section 2.1 it was explained that the wave field in the vicinity of a large pile is transformed by reflection and diffraction. The resulting wave field is the superposition of incoming, reflected and diffracted waves. The characteristics of these waves are understood well. Therewith MacCamy and Fuchs (1954) developed a theory to determine the wave motion around a circular cylinder (see Section 4.3.2, Appendix D). Their model resulted in a phase-resolved flow. This seemed correct since in an undisturbed flow of waves the water particles move oscillatory on epileptically orbits. In 1997 Sumer and Fredsøe identified that in the disturbed flow around a large pile the motion of water particles shows cycle-to-cycle variations. The measurements of Sumer and Fredsøe are given in Figure 4-5. For the point P in the vicinity of the pile the radial and tangential velocities were measured. In the diagram the time series of several wave cycles are plotted on top of each other.
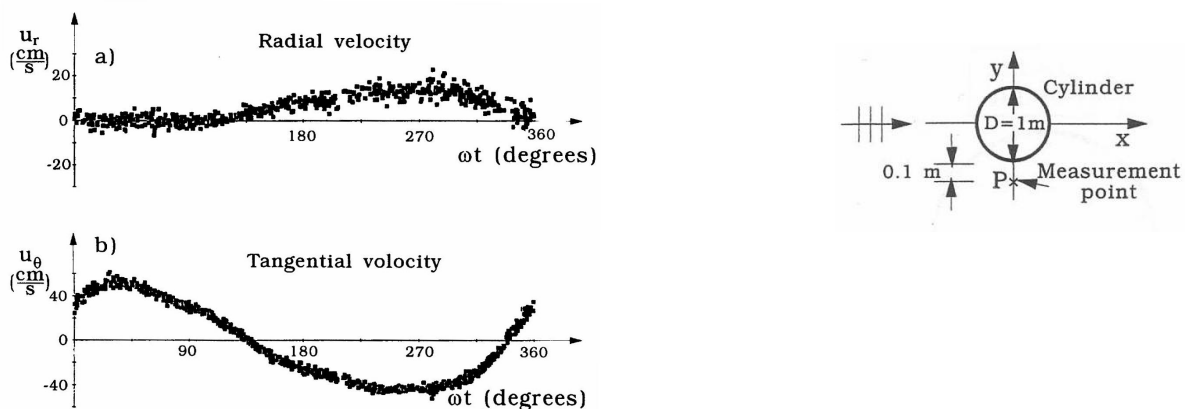
Figure 4-5: Time Series of the radial (a) and tangential (b)   velocity at point P (0.4 cm above the bed, KC = 1.1, D/L = 0.15) (Sumer and Fredsøe, 1997)

Comparing the area between the curve and the horizontal axis for both directions it is obvious that the flows are not equal. The cycle-to-cycle variation of the water particles is illustrated on the left side of Figure 4-6.
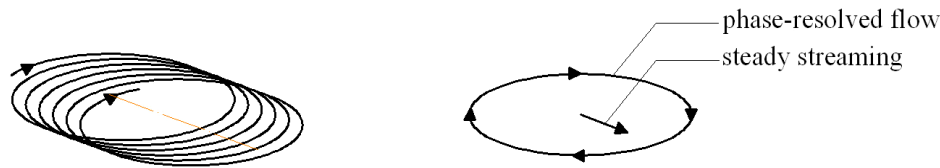
Figure 4-6: Illustration of the phase to phase shift and its division into a phase-resolved flow and
            a steady streaming

Sumer and Fredsøe interpreted the wave induced flow around a pile in the diffraction regime as a phase-resolved flow superposed with a steady streaming. This is visualized on the right side of Figure 4-6. In the following two subsections the form of the phase-resolved flow and the steady streaming is reported and analysed separately in the same way as it has been done by Sumer and Fredsøe (1997, 2001b, 2002).

a) Phase-resolved flow

Figure 4-7 displays the velocity measurements of the phase-resolved flow by Sumer and Fredsøe (1997) in the horizontal plane. A radial flow around the pile is visible. The amplitude of the velocity is maximal at the sides of the pile. In the front and lee the velocity is nearly zero. Sumer and Fredsøe detected that in the vicinity of the pile the amplitude of the velocity is increasing to more than double of the velocity of the undisturbed flow.
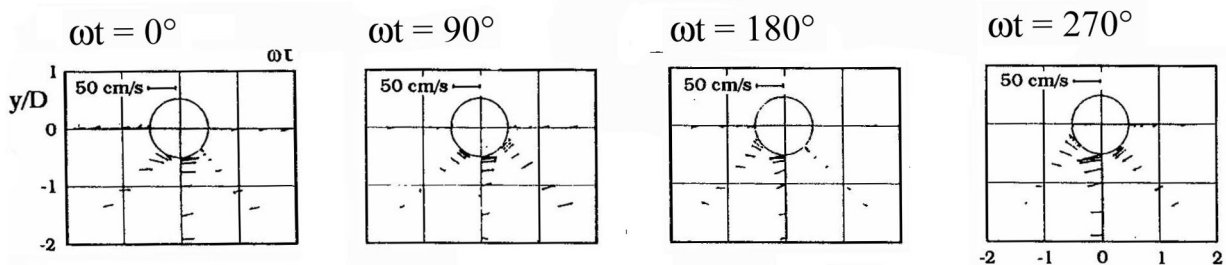
Figure 4-7: Phase-resolved flow (Sumer and Fredsøe, 1997)

The illustrated horizontal velocities should be interpreted as a 2 dimensional orbital motion like under undisturbed waves. This is illustrated in Figure 4-8.
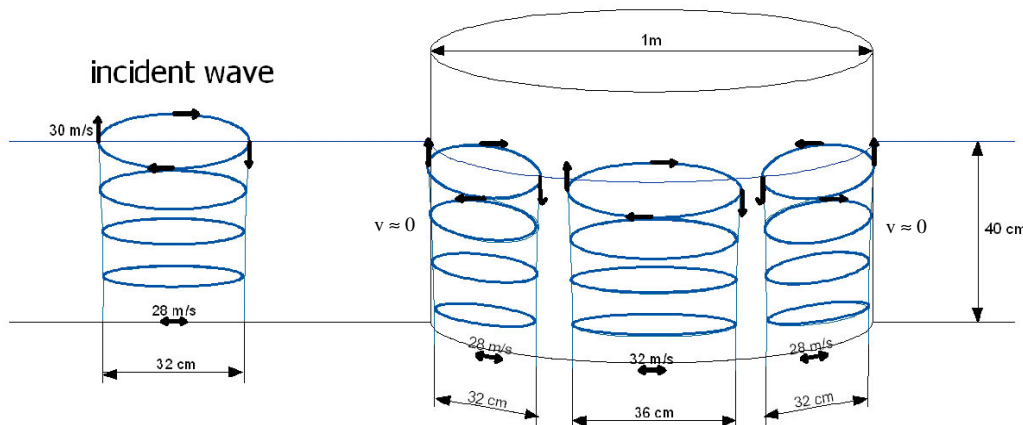
Figure 4-8: 3-dim. idea of the phase-resolved flow

Comparing the cycle-to-cycle variation with the amplitude of the velocities in Figure 4-5, it is apparent that the maximum velocity of the phase-resolved flow is much larger than the velocity of the steady streaming. Therewith the phase-resolved flow has a large influence on the up stirring of the sediment particles. The cycle-to-cycle variation or "steady streaming" has a considerable effect on the scour development as well, because by the phase-resolved flow the lifted sediment particles can not be washed away. In the next subsection the character of the steady streaming is explained.

b) Steady-streaming

The velocity of the steady streaming is defined as the averaged velocity over the wave period:

$$U(z) = \frac{1}{T} \int_0^T \overline{u}(z,t)\, dt \tag{4.1}$$

An example of a time series of the velocity u(z,t) was introduced in Figure 4-5.

Sumer and Fredsøe (2001b) have made extensive model tests to determine the steady streaming around a large pile. In Figure 4-9 the velocity and shape of the steady streaming, as measured by Sumer and Fredsøe (2001b), are depicted. The velocities are shown only in the horizontal plane, because the vertical velocities were not measured.

On the first look it is strange that the steady streaming is mostly directed against the direction of the waves. This can be understood by examining the origin of the steady streaming. A streaming is the consequence of pressure differences. The pressure distribution is generated by the diffracted wave field. Following Figure 4-4 the wave height is high at the side of the cylinders and smaller in the front, so that a phase-to-phase shift occurs towards the low pressure area in front of the pile. This need to be understood under consideration that the wave field are different in dependence on the wave characteristics and the size of the pile (see Section 4.1.1 and 4.1.2).
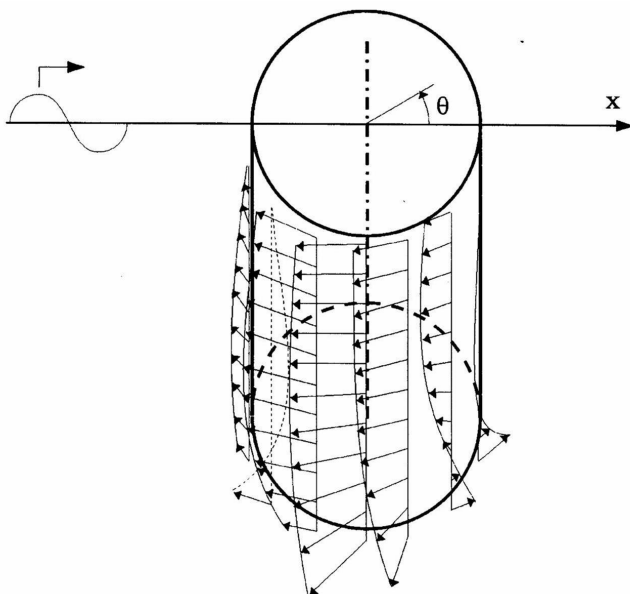
Figure 4-9: Experienced horizontal velocities of the steady streaming

The radial velocity at the boundary of the pile must be zero. The measured radial velocities close to the pile however are clearly not zero. This indicates the existence of a vertical steady streaming. The vertical velocities in the vicinity of a large pile haven't been measured until now.

Sumer and Fredsøe (2001) recognized that the standing wave in front of the pile is similar to a standing wave in front of breakwaters. The flow characteristics in front of breakwaters is shown in Figure 4-10. As can be seen in Figure 4-10 the streaming under the crests of the waves is directed downwards and towards the troughs of waves. Under the trough the streaming is directed upwards. At the antinodes crest and trough alternative, while at the nodes the elevation stays zero. The streaming processes can be understood by the pressure differences and is therewith adaptive on the wave field around a large pile.
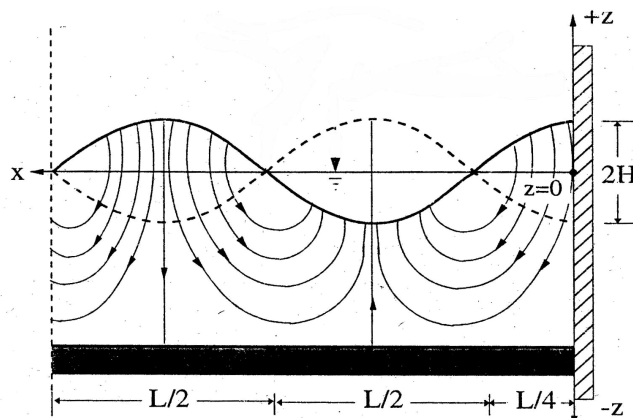
Figure 4-10: Streaming in front of a vertical breakwater (Oumeraci, 1996)

Sumer and Fredsøe (2001) observed a cycle to cycle variation in this flow as well, leading to a vertical flow as shown in Figure 4.11.
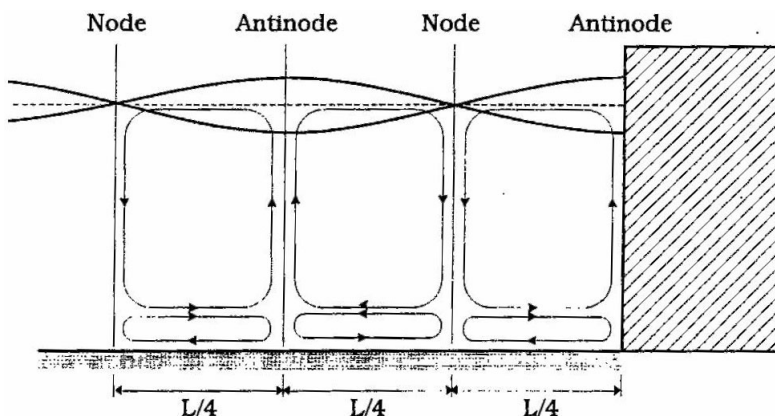
Figure 4.11: Steady streaming in the vertical plane in front of a vertical breakwater (Sumer and Fredsøe, 2001)

The scour process is influenced by the streaming near the sea bed of the flow. Due to the upstream under the nodes scour is formed here, while accumulation is formed under the antinodes.

The flow and scour processes in front of a breakwater is not exactly the same. The surface of the pile is rounded and therewith the waves can space out in a larger area, shaped like a trapeze. Nevertheless by the insight in the flow and scour processes in front of breakwater

scour processes around a pile in the diffraction regime can be understood better. The idea of the vertical flow and their influence on the scour topography is shown in Figure 4.12.
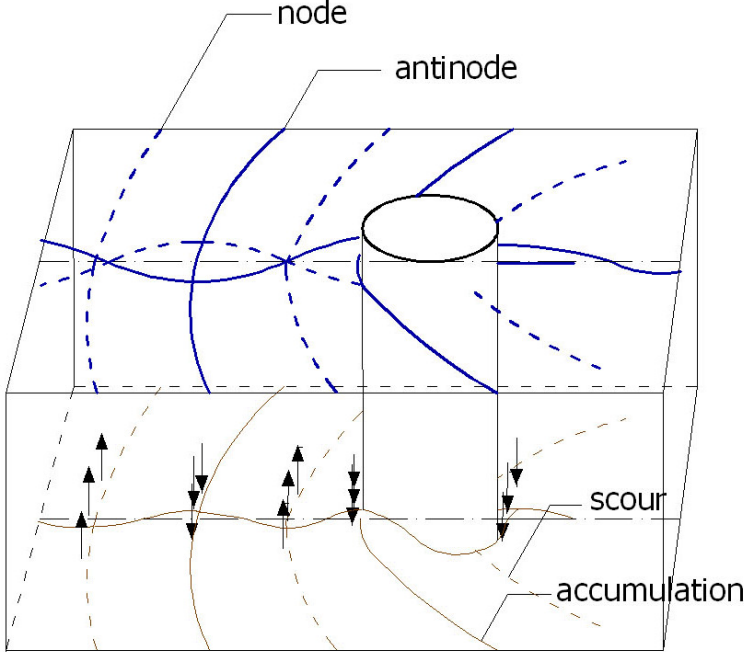
Figure 4-12: Vertical flow due to the diffracted wave field

4.2   Scouring – empirical evaluation

In the previous section it was explained, that the diffraction dominated flow regime, hence the flow around large and intermediate piles, is not understood in detail. Partly it can be modelled analytically (see Section 4.3). No analytical prediction of the equilibrium scour depth is developed, nor does a general excepted empirical formula exist. However, large diameter structures are built and therefore a satisfactory scour prediction needs to be found.

In Section 4.2.3 the prediction of a maximal scour depth is discussed, therefore an overview of performed model tests and their results is provided in Subsection 4.2.1 and a summary of predictions found in literature is given in Subsection 4.2.2.

Beside the equilibrium scour depth, also the scour extension and the time-scale of scour is looked at. The extension of the scour is of interest for the design of a scour protection. The time-scale of scour need to be considered for the discussion of backfilling (Section 5.3). It is advantageous by determining a maximal time-limited scour hole due to varying tidal currents or during the construction.

The reader is referred to the following linked sections:
  Section 5.1: Summary of conclusion of Chapter 4
  Section 5.2: Uncertainties in scour predictions
  Section 5.3: Application to offshore wind turbines

4.2.1   Model results

In Table 4-2 experiments, carried out at large piles, and their results are summarized. The colours refer to the flow regimes (yellow: diffraction regime, blue: intermediate regime). Unfortunately only the equilibrium scour depth of Sumer and Fredsøe (2001) and Zhao et al. (2004) were published (Table 4-2). The other experiments are listed to present an overview for which conditions experiments were carried out. Their conclusions are listed in the last column.

To get a first idea of the experimental results and statements of scour prediction (see Section 4.2.2) an illustration is given in Figure 4-12. Following Sumer and Fredsøe (2002) the experimental results as well as the predictions (as far as possible) are illustrated over the Keulegan-Carpenter number KC and the diffraction factor $^D/_L$. In Section 2.1 it was defined that diffraction is significant for $^D/_L > 0.1$. Lee-wake vortices occur for KC > O(1).

The results of Sumer and Fredsøe (2001b) and Zhao et al. (2004) can not be compared directly, because Sumer and Fredsøe investigated wave only conditions and Zhao et al. investigated wave and current conditions. The current velocity is shown by the numbers next to their results. The illustration might not be clear in each detail, but gives an overview of the available empirical data. The detailed evaluation of the results and empirical based statements (Section 4.2) is described in Section 4.2.3.

Table 4-2: Model experiments on large piles

a.) experiments published with equilibrium scour depth

	D [cm]	h [cm]	T [s]	H [cm]	L [m]	v [cm/s]	d50 [mm]	D/L [-]	KC [-]	S [mm]	S/D [-]	special conditions	conclusions
Sumer and Fredsøe (2001)	100	40	3.5	12.0	6.79	0	0.2	0.15	1.10	47	0.047		shape of steady streaming
Sumer and Fredsøe (2001)	100	40	3.5	8.6	6.79	0	0.2	0.15	0.76	39	0.039		influence of KC, D/L
Sumer and Fredsøe (2001)	100	40	3.5	4.9	6.79	0	0.2	0.15	0.43	15	0.015		
Sumer and Fredsøe (2001)	100	40	2.0	8.2	3.7	0	0.2	0.27	0.43	38	0.038		
Sumer and Fredsøe (2001)	100	40	3.5	2.5	6.79	0	0.2	0.15	0.30	8	0.008		
Sumer and Fredsøe (2001)	100	40	3.5	5.7	6.79	0	0.2	0.15	0.55	20	0.020		
Sumer and Fredsøe (2001)	100	40	3.5	6.4	6.79	0	0.2	0.15	0.61	25	0.025		
Sumer and Fredsøe (2001)	54	40	3.5	8.7	6.79	0	0.2	0.08	1.40	18	0.033		
Sumer and Fredsøe (2001)	54	40	3.5	6.9	6.79	0	0.2	0.08	1.20	10	0.019		
Sumer and Fredsøe (2001)	54	40	3.5	6.9	6.79	0	0.2	0.08	1.20	13	0.024		
Sumer and Fredsøe (2001)	54	40	3.5	6.4	6.79	0	0.2	0.08	1.10	2	0.004		
Sumer and Fredsøe (2001)	54	40	3.5	5.6	6.79	0	0.2	0.08	0.98	5	0.009		
Sumer and Fredsøe (2001)	153	40	3.5	12.0	6.79	0	0.2	0.23	0.68	25	0.016		
Sumer and Fredsøe (2001)	153	40	3.5	8.7	6.79	0	0.2	0.23	0.49	18	0.012		
Sumer and Fredsøe (2001)	153	40	3.5	6.9	6.79	0	0.2	0.23	0.41	8	0.005		
Sumer and Fredsøe (2001)	153	40	3.5	6.4	6.79	0	0.2	0.23	0.38	3	0.002		
Zhao, Teng, Li (2004)	66.7	16.7	0.84	3.22	0.91	10.06	0.12	0.74	0.11	7.4	0.011		new numerical model,
Zhao, Teng, Li (2004)	66.7	16.7	0.85	4.18	0.91	10.06	0.12	0.73	0.14	7.5	0.011		shape of the scoured area
Zhao, Teng, Li (2004)	66.7	16.7	0.87	5.06	0.95	10.06	0.12	0.71	0.18	10	0.015		changes in dependence on the
Zhao, Teng, Li (2004)	66.7	16.7	0.88	5.87	0.97	10.06	0.12	0.69	0.21	13.1	0.020		diameter
Zhao, Teng, Li (2004)	66.7	16.7	0.87	6.83	0.95	10.06	0.12	0.70	0.24	12.4	0.019		
Zhao, Teng, Li (2004)	66.7	16.7	0.89	3.32	0.97	4.23	0.12	0.68	0.12	1.2	0.002		
Zhao, Teng, Li (2004)	66.7	16.7	0.89	4.14	0.98	4.23	0.12	0.68	0.15	1.5	0.002		
Zhao, Teng, Li (2004)	66.7	16.7	0.90	5.70	0.99	4.23	0.12	0.67	0.21	5.5	0.008		
Zhao, Teng, Li (2004)	66.7	16.7	0.89	7.06	0.98	4.23	0.12	0.68	0.26	5.3	0.008		
Zhao, Teng, Li (2004)	66.7	16.7	0.84	5.06	0.91	10.1	0.12	0.40	0.17	7.5	0.021		
Zhao, Teng, Li (2004)	36	16.7	0.87	5.08	0.95	7.0	0.12	0.38	0.18	4.5	0.013		
Zhao, Teng, Li (2004)	36	16.7	0.89	5.08	0.97	4.23	0.12	0.37	0.18	1.8	0.005		
Zhao, Teng, Li (2004)	20	16.7	0.87	5.06	0.95	10.06	0.12	0.21	0.18	7.3	0.037		

b.) experiments published without equilibrium scour depth

	D [cm]	h [cm]	T [s]	H [cm]	L [m]	v [cm/s]	d50 [mm]	D/L, KC unknown, h/D =	KC [-]	S [mm]	S/D [-]	special conditions	conclusions
Torsethaugen (1975) (acc.to Whitehouse, 1998)	0.75	0,1 - 0,15	?	?	?	0	?	?	?	?	0.2-1		
Rance (1980) (acc.to Sumer and Fredsøe, 2002)	46.2	?	?	?	?	?	?	?	?		0.032	waves only	S < 0.06 D
											0.064	wave and current	
Katsui et al. (1988)	117	30	0.8	6	0.96	0	?	1.22	0.05	0.58	< 0.04		
Katsui et al. (1988)	117	30	1.0	7	1.40	0	?	0.84	0.10	0.58	< 0.04		
Katsui et al. (1988)	117	30	1.5	8	2.34	0	?	0.50	0.24	0.58	< 0.04		
Katsui et al. (1988)	117	30	2.0	9	3.26	0	?	0.36	0.4	0.58	< 0.04		
Saito et al. (1990)	52.2	16.5	0.94	6.7	1.01	0	?	0.49	0.33	0.2			1st numerical model
Saito et al. (1990)	52.2	16.5	0.94	7.9	1.01	0	?	0.49	0.39	0.2			
Saito (1992)	52.2	11.5	1.02	9.4	1.00	0	?	0.52	0.72				
Touei et al. (1992)	117	30	1	10	1.37	0	?	0.85	0.14	0.15		smooth bed	numerican model of mass
Touei et al. (1992)	117	30	2	10	3.26	0	?	0.36	0.43	0.15		smooth bed	transport and sand movement,
Touei et al. (1992)	117	30	1	10	1.37	0	?	0.85	0.14	0.15		sand ripples	interaction of mean current and
Touei et al. (1992)	117	30	2	10	3.26	0	?	0.36	0.42	0.15		sand ripples	rippled sand bed
Kobayashi (1994)	4.8	10	1.5	3.8	1.44	0	0.6	0.03	5.2	5	0.104		shape of vortices and their influence on the bed topography
Sumer and Fredsøe (1997)	100	40	3.5	12	6.79	0	0.2	0.15	1.1	>4mm	0.037		phase-to-phase shift

regime 2 | 1 < KC < 6
regime 3 | KC < 1
grey numbers indicate values that were calculate by the linear wave theory
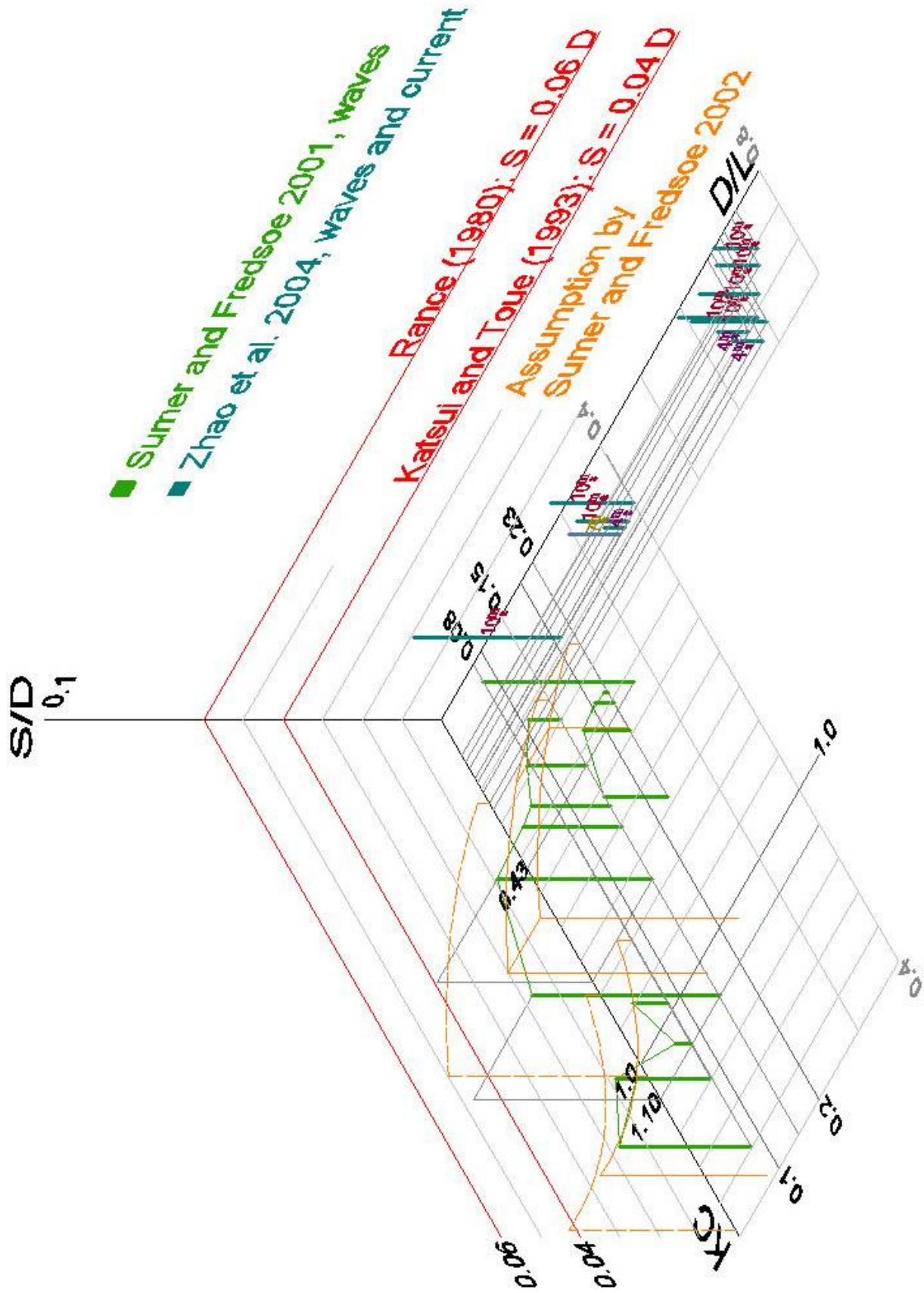
Figure 4-13: Visualization of results of experiments under consideration of S/D = f(D/L, KC)
The numbers next to the results of Zhao et al. give the applied current velocity in [cm/s]

4.2.2   Published scour prediction in literature

a) Parameters

During the last ten years Sumer and Fredsøe did extensive research on the scour around piles in the diffraction regime. Thereby they recognized that the scour depth mostly depends on the Keulegan-Carpenter number KC, the diameter-wave-length-index $^D/_L$ and the Shields parameter θ. Furthermore the Reynolds number of the bottom boundary layer Re_δ, the Reynolds number of the pile boundary layer Re_D and the ratio of the amplitude of the orbital motion to the diameter of the sediment grains $^a/_d$ have an influence on the scour process at large piles.

> Main parameters: KC, $^D/_L$, θ
> Further parameters: Re_δ, Re_D, $^a/_d$

This will be discussed in Section 4.2.3.

b) Equilibrium scour depth

Sumer and Fredsøe (2002) evaluated 16 experiments with regard to the main parameters KC and $^D/_L$. This is shown in Figure 4-13 (left box). The lines through the results give their assumption of the equilibrium scour hole (see Appendix C). Sumer and Fredsøe define the relative scour depth $^S/_D$ in dependence on KC and $^D/_L$. They assume live-bed conditions, wave only loading and an Ursell parameter U<15.
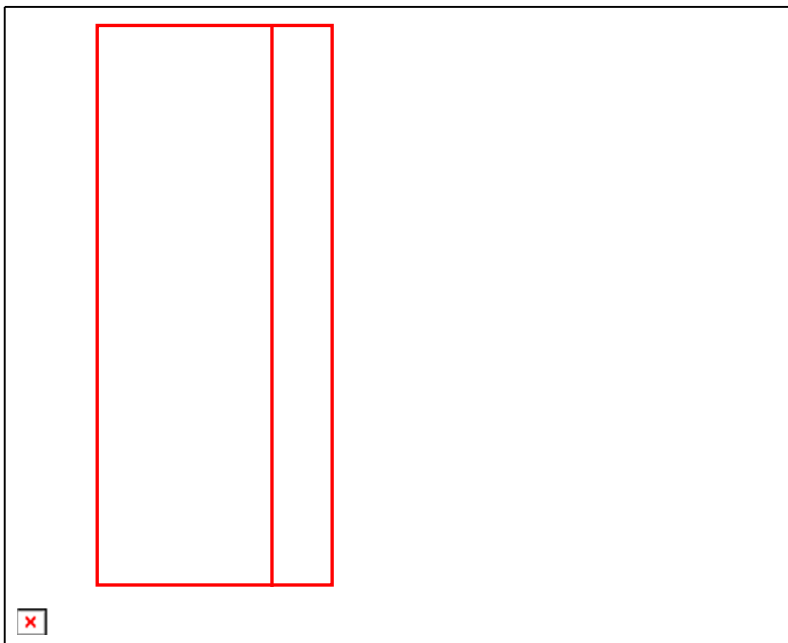
Figure 4-14: Maximal Scour depth in the diffraction regime according to Sumer and Fredsøe (2002)

On the right side of Figure 4-13 the scour estimation for slender piles is shown (Eq. 3.1). As indicated in the middle, no statements about the equilibrium scour depth in the intermediate flow regimes are proposed by Sumer and Fredsøe. The boundaries between the regions are equivalent to the defined flow regimes on which this thesis based (Section 2.1).

Figure 4-12 shows the prediction in a 3-dimensional drawing together with other assumptions and model results. The prediction by Sumer and Fredsøe (2002) is the most recent assumption of the maximal scour depth at large piles. It is the only attempt which also considers other parameters than the pile diameter.

As mentioned, no generally accepted prediction exists. Katsui and Toue (1993) stated that the scour depth is maximal **0.04 %** of the pile diameter. In the summary by Hoffmans and Verheij (1997) it is stated that the scour depth for KC < 6 (intermediate flow regime) is "nil". For piles in the diffraction regime it is referred to Rance(1980) who stated that the scour depth is **0.06 D**. Whitehouse refers to May and Wiloughby(1980) who estimated the equilibrium to be between **0.1 < h/d < 3.**

The different approaches of predicting the maximal scour depth are summarized in Table 4-3. Since there is no general agreed definitions of large piles, the definitions made for each study are given as well.

Table 4-3: Summary of scour predictions in the diffraction regime

	Maximal scour depth	Definition of large piles
May and Wiloughby (1980)	$3\,^h/_d$	D/L > 0.2, h/D < 2
Rance (1980)	$0.06 \cdot D$	D/L > 0.1
Katsui and Toue (1993)	$0.04 \cdot D$	KC < 0.5
Verheij and Hoffmans (1997)	"nil"	KC < 6, D/L < 0.1
Sumer and Fredsoe (2002)	$0.03 \cdot D$	KC < 1.2, D/L < 0.27

No predictions directed to the intermediate pile regime exist. However, the definition of large piles in literature sometimes overlap with the definition of intermediate piles in this thesis. For example the definition of Rance (1980) refers to piles with a diffraction coefficient $^D/_L$ larger than 0.1 and Verheij and Hoffmans (1997) to piles with a Keulegan-Carpenter number KC < 6 and D/L < 0.1. These two definitions together cover the whole intermediate regime.

c)   Time-scale

Sumer and Fredsøe (2002) observed that the time development of scour around large piles is similar to slender piles. Eq. (3.3) is applicable to scour at large piles, but the dimensionless time-scale factor T* is not ascertained well. Evaluating the time-scale measurements of six experiments, Sumer and Fredsøe (2002) resulted in dimensionless time-scale factors between 0.15 and 0.04.

To get an idea about the time scale around large piles, laboratory observations are converted to a pile with a diameter of 4 meter. The used rule of similarity is given by Eq. (4.1).

$$T_N = \frac{1}{\lambda_T} T_M \qquad\qquad (4.1)$$

$$\lambda_T = \sqrt{\lambda_L} = \sqrt{\frac{L_M}{L_N}}$$

(Kobus, 1978 according to Ungruh and Zielke, 2003)

with T_N : measure of time in the nature
        T_M : measure of time in the model
        λ_T : scale factor of time
        λ_L : scale factor of lengths
        L_M : length in the model
        L_N : length in the nature

Sumer and Fredsøe (2001b) measured the time development precisely. In an experiment it took 150 minutes to develop the equilibrium scour by a pile diameter of 1 meter. This results in a time scale of 6 hours at a pile with a diameter of 4 meters.

Saito and Shibayama (1990) performed experiments with a pile diameter of 52.5 centimetres and observed that the equilibrium scour depth was formed after 4 hours. The declaration in whole hours indicates that their observation of the time-scale is likely to be less exact than Sumer and Fredsøe (2001b). For a pile with diameter of 4 meter the time-scale according to Saito and Shibayama (1990) result in 11 hours.

d) Extension of the scour hole

To design the scour protection appropriately and to determine its costs, it is necessary to know the maximal scour extensions. Rance (1980) stated that the scour around large piles occurs in a radius of up to 0.75 times the pile diameter. No further experiences about the maximal extension of the scour hole are given in literature. From published scour hole topographies it can be stated, that the assumption by Rance underestimates the maximal scour extension. The two scour holes measured by Sumer and Fredsøe (2001), which are shown in Figure 4-2, are examples. The pile diameter is 1m. On the left figure the scour hole in front of the pile extends 1 meter. In the right figure the scour hole at the side extends 1 meter as well. In Subsection 4.1.2 it was explained, that the extension of the scour hole is likely to depend on the wave length.

4.2.3   Appraisal of the statements

On the basis of the experimental results (Section 4.1.1) and the understanding of the flow regime (Section 4.1), the available predictions, which were summarized in the previous section, should be discussed.

a) Coherences between parameters:

Sumer and Fredsøe (2001) stated that the scour development around large piles mostly depends on the Keulegan-Carpenter number KC, the diffraction factor $^D/_L$ and the Shields parameter θ. The Shields parameter (see Section 2.2.2) is related to the soil conditions as a parameter to determine the initiation of motion. Its influence on sediment transportation is beyond dispute. The other two parameters describe relations between the character of the wave and the diameter of the pile (see Appendix A).

Since both parameters include the diameter of the pile, it is started with analysing the influence of the pile diameter on the flow and therewith scour. Afterwards the influences of KC and $^D/_L$ are discussed under consideration of the flow characteristics and the model results, as well as the background understanding, which was explained in Chapter 2.

Pile diameter D:

KC and $^D/_L$ both contain the pile diameter D. Whereas $^D/_L$ is proportional to D, KC is antiproportional to D.

Increasing the pile diameter by leaving all other influences unchanged, the hindrance of the flow increases. The diffraction and reflection of the waves become stronger. This causes a heightening of the maximal velocity of the phase resolved flow.

By a larger hindrance the flow lines of the current will contract stronger, so that the current velocity is increased by an increasing diameter as well.

A steady streaming does not exist in the absence of the pile. By increasing the pile diameter it is most likely that the steady streaming increases as well.

Recapitulating, all involved flows increase by an increasing pile diameter D. An increasing pile diameter by constant wave conditions leads to an increase of the diffraction factor $^D/_L$ and a decrease of the Keulegan-Carpenter number KC.

Keulegan-Capenter number KC:

Observing the experimental results of Sumer and Fredsøe (2001) in Figure 4-12 the increase of the relative scour depth $^S/_D$ by the rise of KC is obvious. Physically it can be understood by considering the diameter of the pile to be constant:

$$D = const$$

$$\frac{S}{D} = f(KC) = f(const^{-1}U_m T_w)$$

The heightening of KC caused by a constant pile diameter means the increase of the maximal orbital velocity (and wave period). This surely leads to a higher loading of the sand grains on the sea-bed and an increase of lifted sand grains (see Section 2.2).

Diffraction factor $^D/_L$:

Scouring around large and intermediate piles is dominated by diffraction. $^D/_L$ is a parameter to describe diffraction, so there should be a strong relation. Observing the experimental results of Sumer and Fredsøe (2001) however does not show the relation between $^D/_L$ and $^S/_D$ clearly: The relative scour depth of $^D/_L = 0.15$ is larger than the relative scour depth of D/L = 0.08 with comparable KC, but also larger than comparable values for D/L = 0.23 (see Figure 4-12).

Sumer and Fredsøe deduced their statement by the observation of the maximal orbital velocity on the bed. Their illustration is given in Figure 4-14. The amplitude of the orbital velocity increases with increasing $^D/_L$.
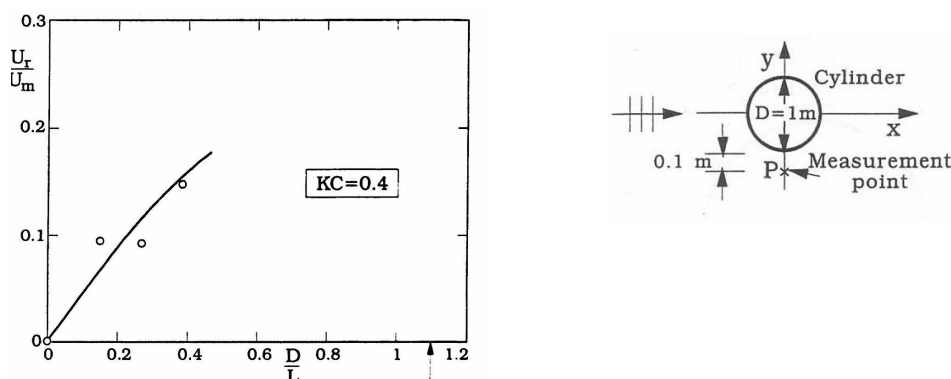
Figure 4-15: Radial component of the period averaged (steady streaming) velocity at point P,
         z = 0.4cm, KC = 0.4 (Sumer and Fredsoe, 2001)

The experimental data in Table 4-3 show, that in the experiments of Sumer and Fredsøe (2001) T and L were constant. These wave parameters were only varied in the experiment with $^D/_L$ = 0.27. The diffraction factors $^D/_L$ of the other experiments differ only by the variation of the pile diameter D. The influence of the pile diameter was already discussed in the beginning of this section. With an increasing diameter the scour depth increases, as well as the diffraction factor $^D/_L$. The results of Sumer and Fredsøe do not show, that the increase of the diffraction factor generally means an increase of the scour depth, because the influence of the variation of the wave length is not well considered and the wave length might be related to further parameters and processes.

First the experimental results of Zhao et al. (2004) will be evaluated towards the influence of the diffraction factor. Afterwards its influence is discussed based on the flow characteristics.

The experiments of Zhao et al. (2004) were carried out in an area with relatively small Keulegan-Carpenter numbers KC ≤ 0.26. From Sumer and Fredsøes experiments it can be derived, that the dependency on KC is small in these experiments. The results of Zhao et al. (2004) in relation to $^D/_L$ are illustrated in Figure 4-15.

The results show, that the relative scour depth decreases with increasing diffraction factor. This is in contradiction with Sumer and Fredsøe's statement. The models vary on the pile diameter and wave length.
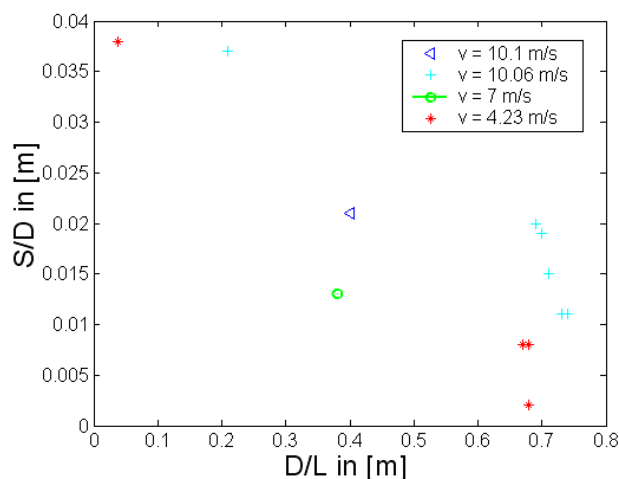
Figure 4-16: Relative scour depth $^S/_D$ in relation to the diffraction factor $^D/_L$ (results of Zhao et al., 2004)

The influence of the diffraction factor $^D/_L$, the influence of a changing wave length under a constant pile diameter and wave height can be explained as follows. A decreasing of the wave length changes the diffracted wave field. The distances between crests and troughs increase. Therewith the distances between high and low pressure increase. This influences the steady streaming and the current, which was only existent in the tests of Zhao et al.

The influence of the diffraction factor $^D/_L$ is not clear. Under consideration of a constant D an increasing $^D/_L$ is equivalent to the decreasing of the wave length.

Current:

Analog to slender piles the existence of a current increases the scour. It is likely that the influence of the current related to the time-scale is substantial large, because the current has a high transport potential to wash away the lifted sand particles. The order of the influence on the equilibrium scour depth can be seen by the model results of Zhao et al. (Figure 4.15).

b) Equilibrium Scour Depth

Estimation of the equilibrium scour depth in the diffraction regime (large piles):

The insight in the coherences of the parameters is too little to predict the scour in relation to the Keulegan-Carpenter number KC or the diffraction parameter $^D/_L$. An overall prediction for the whole regime is more reliable. In Figure 4-12 28 experimental results are confronted with the predictions found in literature. The maximal scour depth is related to KC = O(1). In this region only results due to wave action are in hand. For the wave only condition the estimation by Rance (1980) is recommendable as upper limit: Following Rance the scour depth is less than 6% of the pile diameter.

By Richwien and Lesny (200b) and the report of the annual report of the German Bundesanstalt für Seeschifffahrt und Hydrographie (2004) the surface currents in the German North Sea are predicted as less than 2 $^m/_s$. The impact of the currents is estimated by the experiments of Zhao et al. (2004) with a current velocity of 4 m/s and their relation to Sumer and Fredsøes (2001b) wave only experiences. Thereby the author recommends assuming the maximal scour depth under offshore conditions to 10% of the pile diameter.

For the application in reality, a safety factor for insecurities needs to be added. Insecurities are discussed in Section 5.2.

From experiences with slender piles, as well as the analysis of the prototypes in Section 5.2.2, it is known, that the maximal scour depth under breaking waves is not included in the set limits. Erecting a large pile in a zone, the maximal scour depth can be estimated from research about scour in front of breakwater. Therefore it is referred to Sumer and Fredsøe (2002).

Estimation of the equilibrium scour depth in the intermediate regime:

Scouring in the intermediate regime is hardly investigated. However the maximal scour depth can be predicted in some parts of the regime. This can be evaluated best by Figure 2-6, which illustrated the occurrence of vortices and the significance of diffraction in dependence of KC and $^D/_L$. For a better understanding it is explained in more detail here. In green the conclusion are added.
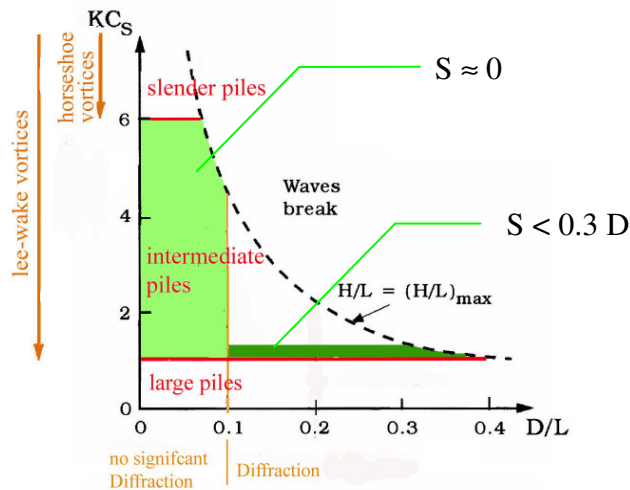
Figure 4-17: Prediction of equilibrium scour depths in the intermediate regime

Hoffman and Verheij (1997) declared that for $^D/_L < 0.1$ and KC < 6 the scour depth is nil. This is reasonable. The wave motion is so weak, that no significant diffraction is formed. The prediction of scour around slender piles (Sumer et al., 1992, see Figure 3-1 and Eq. 3-1) indicates that the existing lee-wake vortices are too weak to cause relevant scour.

In the area of KC = 1.1 accumulation behind pile is formed (see Figure 4.2a), so lee-wake vortices do not have large influence in this area. The experimental results in Figure 4-12 showed no unsteadiness at the boundary to the intermediate flow regime, but a further increasing of the relative scour depth. For conditions O(1) < KC < O(1.4)[2] the limits of large piles are taken over. Observing the illustrated conclusions in Figure 4-16, there is an area left for which no predictions were made. In the left area significant diffraction occurs. Weak lee-wake vortices exist as well and they might have an influence on the streaming. No experiments have been published about this area, so that the order of scour can not be predicted. Designing a structure a high scour depth like 1 to 1.5 times the diameter must be considered or model tests need to be performed.

Analog to slender and large piles the maximal scour depth in the case of breaking wave can be much higher.

---

[2] Sumer and Fredsøe (2002b) investigated piles up to KC = 1.4.

4.3   Scouring – theoretical estimation

Theoretical models to evaluate the velocity around a large circular pile do exist. Toue and Katui (1992) and Zhao et al. (2004) presented attempts of modelling the whole scour processes around large piles. Therefore the sub-models are built up: wave model, current model and a sediment transportation model. The evaluation of such a over-all model requires a high effort of calculation. The effort as well as the result would exceed the scope of this thesis. To proof the order of the maximal scour depth and to obtain the order of the forces acting on a scour protection around a large diameter pile, the submodels are reviewed and evaluated towards the maximal velocity at the sea-bed.

4.3.1   Wave model

In Section 2.1 it was explained that large structures disturb the wave field. Reflection and diffraction occur. These phenomena are well understood. In 1954 MacCamy and Fuchs (1954) presented their model of the wave field around a large vertical cylinder. It basically consists of the superposition of incident, reflected and diffracted wave field. A more detailed explanation is given in Appendix D.

Saito and Shibayama (1990) and Sumer and Fredsøe (1997) confronted their velocity measurements around large diameter piles with the velocity distribution determined by the MacCamy and Fuchs theory. The outcomes of Sumer and Fredsøe (1997) are shown in Figure 4-17.
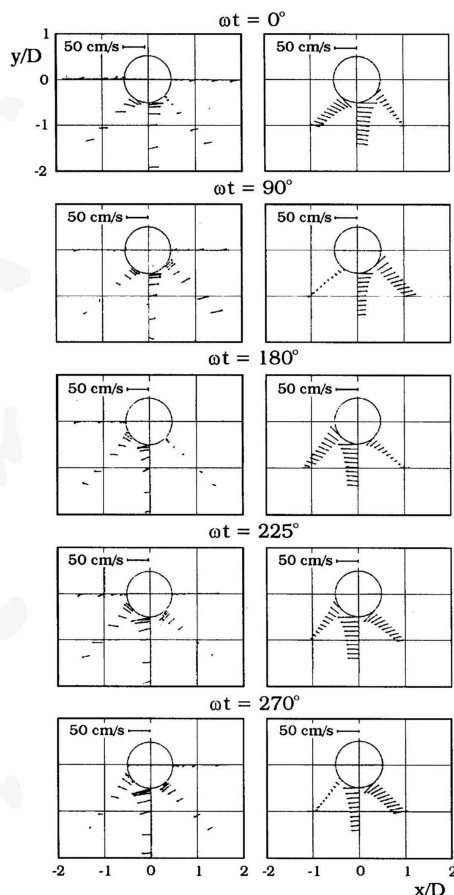
Figure 4-18: Comparision of measured phase-resolved flow and modelled velocities by the MacCamy and Fuchs theory (Sumer and Fredsøe, 1997)

The amplitude of the velocity can be modelled well by the MacCamy Fuchs theory. However Sumer and Fredsøe recognized that the steady-streaming is not evaluated by the MacCamy and Fuchs theory. The evaluation of Sumer and Fredsøe showed that the steady streaming is between 20 and 25% of the phase-resolved flow.

An identified phase-difference between the measured results and the calculated results is not relevant in this result since only the maximal velocity is needed.
Considering the wave characteristics in the nature, the assumption of the linear wave theory, which is included in the MacCamy and Fuchs theory, is another source of uncertainty.
Sata and Shibayama (1990) believe that the inconsideration of the viscosity causes imprecise results if separation (KC > O(1)) occurs.

Recently Zhao et al. (2004) presented a different model of the wave field around large-scale vertical circular cylinders. By using the hyperbolic mild-slope equation they got good results as well. Since this theory is more difficult to evaluate and the MacCamy and Fuchs theory delivers good results, this method is not evaluated.

4.3.2   Current model

Sata and Shibayama (1990) simulated the current around a large diameter pile by integration over the depth by spatial variation of the radiation stress and the mass transport velocity. This would require a high effort of programming and calculation. For the prediction of the order of the maximal scour hole it is sufficient to determine the maximal amplification of the velocity. This can be concluded with the classical hydromechanics with respect to Bernoulli.

As shown in Figure 4-18 the maximal velocity in the vicinity of the pile can be estimated as twice the undisturbed current velocity.
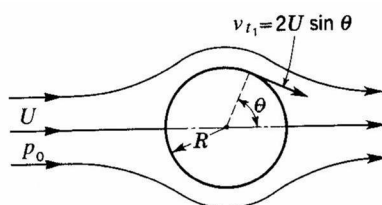
Figure 4-19: Laminar flow around a cylinder by a uniform current (Daugherty et al., 1985)

This simplified approach gives the order of the amplification of the current velocity. This is a sufficient basis for the conclusions in the thesis. The influence of the pressure differences due to the wave field on the current velocity is unconsidered.

Whether the assumption of a laminar flow is right can be evaluated by the Reynolds number. This is explained in Appendix A. For further understanding the book from Daugherty et al. (1985) is recommended.

4.3.3   Interaction of wave and current

In offshore conditions the combination of waves and currents are the most common condition. Superposing the resulting bottom shear-stresses gives good results (Zhao et al., 2004). The definition of bed shear stresses due to constant and cyclic loading were given in Section 2.2.2.

Two constant streamings are to be considered around large piles: The streaming of the current and the steady streaming due to waves.

In the offshore environment the current and waves do not necessarily approach co-direction. Since this research leads to the estimation of the maximal scour hole and maximal loading of scour protection, it is adequate to consider the co-directional case.

4.3.4   Vortices in the intermediate flow regime

In Section 2.1.1 it has been ascertained that in the intermediate flow regime lee-wake vortices occur and influence the scour process. As can be seen in Table 4-1 experiences with this flow regime are hardly available.
Sumer and Fredsøe (2002) stated that the scour development in the intermediate flow regime is dominated by the steady streaming. This is the case in the large pile flow regime as well. The difference is that the lee-wake vortices may have an influence on the steady streaming. No observation due to this conditions where found in literature

4.3.5   Further influences

No experiences with the influences of breaking waves and liquefaction on the scour around large piles were found in literature. As explained in Chapter 3 these effects can essentially increase the scour hole and need to be considered in the implementations and conclusions (Chapter 5 and 6).

5   Implications for Scour Predictability: Example Application for Offshore Wind Turbines

As explained in Section 1.1 the main objectives of this literature research are the predictability of scour at large piles and at monopile-founded offshore wind turbines. By analysing the knowledge about basic scour processes (Chapter 2) and scour at large piles (Chapter 4) the scour prediction at large piles was analysed in Section 4.2. The main conclusions are summarized in Section 5.1. After applying safety factors due to uncertainties (Section 5.2) the knowledge of flow regimes and scour at slender and large piles is applied on wind turbines (Section 5.3). In the end of this chapter implications are drawn for the design of scour protection (Section 5.4). In Figure 5.1 the methodology is illustrated to explain the steps of analysis and its conclusions.

Understanding of scour processes	(2.1, 2.2, 4.1)	**Coherences between parameters** S, D, KC, $^D/_L$ (4.2.3 a)
Results of model tests	(4.2.1)	
Empirical approaches	(4.2.2)	**Equilibrium scour depth** S/D (4.2.3 b)
Scour at slender piles	(3)	
Differences model ←→ reality	(5.2.1)	**Application: Pile design** D, t, € (5.2)
Uncertainties	(5.2.2)	
Designing an Wind Turbine	(2.3)	**Most feasible design** (5.3, 6.3)
Design of Scour Protection	(references)	

Figure 5.1: Approach of the analysis (the numbers in brackets refer to related sections)

5.1   Equilibrium scour at large piles

In this section the most important insight in the scour processes at large piles are summarized with focus on the predictability of scour.
Piles in the diffraction and the intermediate flow regime are discussed. To understand the notation "large" and "intermediate" it is referred to Section 2.1 and Chapter 4. The flow regime can be defined by the Keulegan-Carpenter number KC (see Appendix A) as follows:

KC < O(1)   : large piles   or   diffraction regime
O(1) < KC < O(6) : intermediate piles or   intermediate regime

5.1.1   Diffraction regime

In the diffraction regime the incoming waves are transformed by reflection and diffraction. In the modified wave field around the pile the orbital velocity of the water particles increase up to twice the maximal incoming velocity (Oumeraci, 1996). The incoming current is not only accelerated due to the hindrance, but also influenced by the pressure distribution. As a consequence of the disturbed wave field the pressure distribution is different than in the vicinity of slender piles. Due to the pressure distribution also under wave only conditions a steady streaming is formed around the pile. In wave only conditions this steady streaming has a large impact on the scour processes, because the orbital motion of the phase-resolved flow can not wash away lifted sediment.

The insights in the scour processes are under development. However the influence of the wave length L and therewith of the diffraction coefficient $^D/_L$ are not well understood, neither the influence of currents. Only an overall estimation of the equilibrium scour depth can be made. The recommendation of Rance (1980), who stated the equilibrium scour depth to be less than 6% of the pile diameter, is recommendable for large piles under wave impact. Due to the current impact the equilibrium scour depth offshore was determined to be less than 10%. This prediction is believed to be on the safe side for scour around circular piles in the diffraction regime. For the application of wind turbines, the recommended scour depth, which should be taken into account, is amplified by a factor of 3 to 30% of the pile diameter. This is done because of the specific character of a monopile-founded wind turbine. A wind turbine is showing dynamic motion by which the sea-bed next to the pile is cyclic deformed and therewith loosened.

To ensure a reliable design some indices on smaller equilibrium scour depth were not taken into consideration. The equilibrium scour depth decreases with decreasing Keulegan-Carpenter number. Due to the shape of the wave field scour and accumulation is formed. Under offshore conditions the incoming waves vary in impact and direction. This is likely to cause a partly compensation of scour and accumulation.

5.1.2   Intermediate regime

The intermediate flow regime was defined as a consequence of the overlapping of the conditions which lead to the formation of vortices and the conditions which lead to significant diffraction. At the boundary of slender piles the formed vortices are so weak, that no considerable scour is occurs. This is valid for KC < 6 and $^D/_L$ < 0.1. The vortices become more and more weak up to the other boundary of KC = O(1). For smaller values no vortices occur at all. Close to this boundary the scour can be predicted equal to large piles, hence the relative scour depth $^S/_D$ is:

< 0.06 under waves only condition,
< 0.1   at normal circular piles installed offshore,
< 0.3   at (swaying) offshore wind turbines

On Figure 4.16 it was shown, that there is a region of the intermediate flow regime, were no reliable prediction is possible. Here significant diffraction occurs together with weak lee-wake vortices. No experiences were made under these conditions, so that the impact of the lee-wake vortices under influence of diffraction is unknown.

5.2   Uncertainties

There are different kinds of uncertainties. A model is not an exact replica of the reality. The site conditions can not be predicted exactly for the life-time of a structure and the scour processes are not understood in each detail. In the following three subsections a brief introduction is given of uncertainties in the scour prediction. At the end of this section the empirical scour predictions which were evaluated in Chapter 3 and 4 are discussed and modified for the application.

5.2.1   Application of model results on an actual design

The research of scour around bridge piers, breakwaters or slender piles showed that the experimental results differ from the actual processes offshore. Some of the differences between model and offshore conditions and problems of scaling are listed in Table 5-1.

Table 5.1: Scale and laboratory effects in scour modelling

Model	Reality
Constant conditions	Variation of impacts: - waves - current - water depth
Mostly regular, symmetrical waves	Unregular, unsymmetrical waves
One- directional incident waves	Superposition of waves in different directions
The diameter of the sediment grains is not modelled by the scale factor, because the grain sizes in the model would be so small that cohesion forces are formed. Without modulating the grains according to the scale factor, the relation between the grain diameter and other parameters (e.g. bed roughness) are different in model and reality.	
Mostly plain bed	Rippled bed
Model effects: Similarity can not be achieved in all fields in one model. For example this requires a complete dynamic the similarity of all involved forces (Section 2.2.1). Parameters like acceleration of gravity, density of water, pressure and velocity can not be modelled by the same scale factor.	
Sea growth in reality, backflow due to closed basin in model, loading of the sediment through the lateral loading of the pile, …	

Observing the particular differences, some cause an underestimation of the equilibrium scour depth by model tests and other an overestimation. For instance the equilibrium scour depth under regular, symmetrical waves can be conceived to be smaller than under unregular, unsymmetrical waves. On the other hand, the variation of the current in a tidal wave leads to smaller scour depth offshore than in model tests.

There are also specific model dissimilarities related to offshore wind turbines. As mentioned in Section 2.3 a monopile-founded offshore wind turbine is a dynamic sensitive structure. Even at the height of the sea bed the pile sways over several centimetres. This causes a loosening of the sediment in the vicinity of the pile which remained unstudied in most tests.

5.2.2   Uncertainties in design parameters

Offshore wind turbines are usually planned for a life-time of 20 years. They need to be designed to resist the environmental loading over a lifetime. The actual condition during the next 20 years can not be predicted. Instead recent measured data at the site of the planned wind farm and existing data out of the region are taken and evaluated statistically.

Another uncertainty is the occurrence of global sand waves which can cause a decrease of the maximal scour depth as well as an increase.

5.2.3   Prototype

In-field measurements are helpful to find a relation between laboratory results and reality. These results need to be evaluated carefully to avoid an underestimation of scour. Only recently methods were developed to measure the scour around a pile permanently. A lot of in-field measurements were taken after a storm when the offshore conditions calmed down and a landing by boot was possible again.

In Chapter 1 two measurements of prototypes were shown (Figure 1.2), these should serve to adjust the empirical statements for slender and large piles for practical applications. The underlying calculation is given in Appendix E. Unfortunately only one of the measurements was useful. For the second the wave length is unknown which leads to immense discrepancies in the evaluation.

The scour around a pile of a diameter of 3.5 meters was measured after a storm at the Europlatform, which is located 60km offshore of the harbour of Rotterdam. By the actual storm conditions of this location and the pile diameter of 3.5 meters, a Keulegan-Capenter number of 28 is determined. Therewith scour around this pile must be evaluated with the "slender pile" theory. By the prediction of Sumer et al. (1992) a scour depth of 3.33 meter is predicted. The measured scour depth was 3 meters. The prediction of Sumer et al. (1992) is good. Even if the scour was not measured at the moment of its maximum depth or storm conditions were not exactly estimated, there is a safety margin of 10%.

5.2.4   Conclusion

For the scour prediction around slender piles a prototype measurement could be evaluated. In the area of KC = 28 the prediction can be used without consideration of a safety factor for uncertainties. For a KC of around 10 the prediction is sensitive in relation to KC. The model measurements scatter around the predicted scour depth by Sumer et al. (1992).
A new curve is drawn for the design practice. This is shown in Figure 5.2 (green line). In Section 2.3 it was explained, that offshore wind turbines are dynamic structures. The foundation pile sways with an amplitude of several centimetres. Therefore a second amplification of the design rule of Sumer et al. (1992) is made (red line).
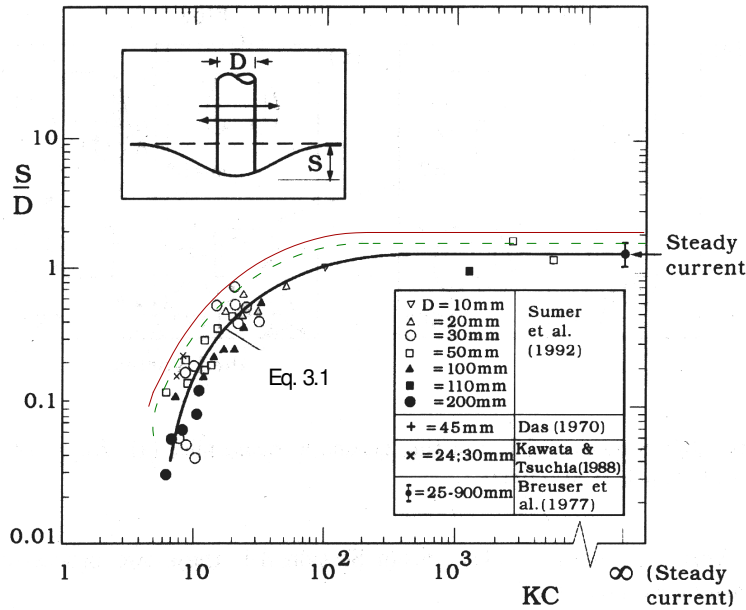
Figure 5.2: Modification of the scour prediction by Sumer et al. for the practical application
(based (black) on Sumer et al. (1992), green – general uncertainties, red – uncertainty due to the
motion of wind turbines)

The applied approach to determine the maximal scour depth around slender piles is simplified. A more extensive sensitivity analysis is recommendable, although not performed here, since the thesis is directed to scour around large piles.

No prototype measurements were available to check the prediction of scour around large piles. In the empirical evaluation (Section 4.2.3) an equilibrium scour depth of less than 10% of the pile diameter was established. This statement includes the uncertainties of scour prediction at large piles. For the application to offshore wind turbines it needs to be considered that the motion of the pile can increase the equilibrium scour depth immense. To avoid an underestimation of the maximum scour depth it is recommended to consider a scour depth of 0.3 times the pile diameter in the diffraction regime.

For piles in the intermediate flow regime the scour is negligible if the diffraction coefficient $D/_L$ is smaller than 0.1 (see Section 4.2.3). Up to a Keulegan-Carpenter number of 1.4 the prediction for large piles can be applied. For the remaining area no reliable predictions can be made.

5.3   Application to offshore wind turbines

In Chapter 3 and 4 empirical evaluation of the equilibrium scour depth for slender, large and, partly, intermediate piles were found or defined. In the previous section they had been modified towards the application of offshore wind turbines.

➢ In the slender-pile regime, which is defined by KC[3] > 6, the equilibrium scour depth should be determined by the modification of Sumer et al.(1992) as shown in Figure 5-2 (red line).

➢ Under KC < 1.4 the equilibrium scour depth is smaller than 0.3 times the pile diameter.

➢ For KC < 0 and $^D/_L$ < 0.1 the scour depth is negligible small.

Beside these design rules, the individual site conditions need to be analysed. In the case of breaking waves, liquefaction or moving sand waves are possible, the risk of the stability failure is increased immense.

In Section 2.3 it was explained, that the stability of a monopile-founded offshore wind turbine is proofed in three separate analyses, hence static analysis, dynamic analysis and fatigue analyses. According to the present design rules one scour depth is dictated for all proofs. The fatigue analysis is usually the design driver.

In this section it is evaluated, whether a distinction between maximal scour depth and usual (average) scour depth is recommendable. The static analysis and the proof of resonance must be verified for the maximal expected scour depth during the life-time of the structure. This is the scour depth related to the once-in-100-years extreme wave conditions. By the fatigue analyses the stability due to the cyclic loading during the whole life-time is proofed. It is sufficient, to consider the average scour hole in this proof.

In the following two subsections the order of the maximal scour depth and the average scour depth is evaluated for several wind farm projects in the North Sea. By the discrepancy the feasibility of the consideration of two different scour depths is shown.

In Section 6.2 the conclusion are summarized.

5.3.1 Maximal scour depth

The maximal scour depth, which needs to be considered in the design of an offshore wind turbine, is the scour depth during survival conditions. The survival conditions are commonly associated with the once-in-100-years case.
To determine the maximal scour depth the monopiles need to be classified according to the flow regimes which were defined in Chapter 2.1 as

KC > O(6)   : slender piles   or   slender-pile regime

KC < O(1)   : large piles   or   diffraction regime

O(1) < KC < O(6) : intermediate piles   or   intermediate regime

For the classification of wind turbines under extreme conditions the maximal water depth, the pile diameter, the wave height and the associated wave period of four example locations are

---
[3] KC := Keulegan-Carpenter number, see Appendix A

summarized in Table 5-2. The examples are sorted in shallow water or near coast conditions (Blyth), common conditions for offshore wind farms (Horns Rev, EWEA) and deep water conditions (German Projects). In water depth up to 25 meters pile diameters between 3.5 to 4.5 meters are common. For large pile diameters, no suitable installation tools are available. As can be seen projects in deeper water conditions with larger diameters are planned, therefore research projects developing larger driving tools and suction piles are running.

Table 5-2: Example Application: Prediction of scour depth at wind turbines under extreme conditions

				h_{max} [m]	D [m]	H_{max} [m]	T (H_{max}) [s]	L [m]	KC [-]	D/L [-]	S/D [-]	S [m]
sha	UK	Blyth	North Sea	8.5	3.5	8	7	50.7	5.7	0.07	1.5	5.3
	DK	Horns Rev	North Sea	14	4	8.1	12	129.4	8.7	0.03	0.4	1.6
common	NL	EWEA (Egmond aan Zee)	North Sea	20	3.5	12.8	9.5	113.3	8.5	0.03	0.3	1.1
				20	3.7	12.8	9.5	113.3	8.0	0.03	0.3	1.1
				20	3.9	12.8	9.5	113.3	7.6	0.03	0.2	0.8
				20	4.1	12.8	9.5	113.3	7.3	0.04	0.2	0.8
				20	4.3	12.8	9.5	113.3	6.9	0.04	0.2	0.9
deep	German Projects in the North Sea, general			40.3	5	23.3	14.5	251	12.3	0.02	1.0	5.0
				40.3	5.5	23.3	14.5	251	11.2	0.02	0.8	4.4
				40.3	6	23.3	14.5	251	10.3	0.02	0.7	4.2
				40.3	6.5	23.3	14.5	251	9.5	0.03	0.4	2.6
				40.3	7	23.3	14.5	251	8.8	0.03	0.4	2.8

For the examples which are still in the designing phase, the pile diameter was varied. All examples show, that offshore wind turbines under extreme wave conditions behave as slender piles. The evaluation of the maximal scour depth is done by the modified prediction of Sumer et al. (1992) (Figure 5-1). For Horns Rev and EWEA, hence water depths between 14 and 20 meters and a pile diameter between 3.5 and 4.3 meters the predicted scour depth are between 0.2 to 0.4 times the pile diameter which is equal to 0.9 to 1.6 meters. A relative scour depth of 0.1 is smaller than the prediction in the diffraction regime. Since the structures are likely to cause significant diffraction for smaller wave heights, the maximal scour depth is 0.3 times the pile diameter. As can be seen in Figure 5-5 the predicted maximal scour depth is 1/3 to 1/5 of the design scour depth dictated by DNV.

The Keulegan-Carpenter number at the near shore example of Blyth classifies the turbine at the boundary between slender and large piles. Following the scour prediction (Section 5.1) no significant scour is to be expected under these conditions. Observing the wave height and water depth however indicates, that breaking waves are likely to occur. In Section 3.4 it was explained, that breaking waves can immensely increase the scour depth. Considering the examples of scour under breaking waves, the maximal scour depth is estimated to be 1.5 times the diameter, which equals the upper limit of the DNV rule (see Figure 5-5).

The evaluation of large diameter wind turbines offshore Germany show, that under corresponding extreme conditions the scour development is dominated by vortices and no significant diffraction does occur. Equal to Horns Rev and EWEA the maximal scour depth is evaluated to be at the lower limit of the DNV rule. The variation of the pile diameter between 5 and 7 meter has a significant impact on the predicted scour depth. The relative scour depth decreases from 1.0 to 0.4 and the actual scour depth from 5 meter to 2.8 meter.

The results are illustrated in three figures known from earlier chapters. Figure 5-3 clarifies the classification under extreme conditions. If no breaking waves are expected the scour depth under extreme conditions can be estimated by the theory about scouring at slender piles. The example of Blyth close below the slender pile regime, is dominated by breaking waves.

In Figure 5-4 is shown, in which area of the slender pile regime the wind turbines were sorted.
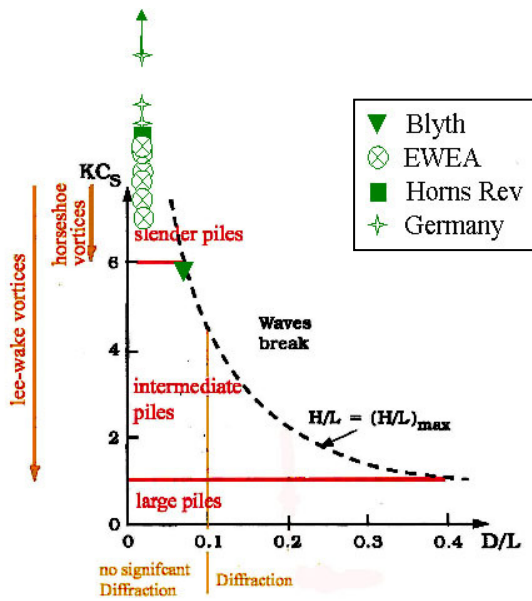
Figure 5 - 3: Classification of wind turbines
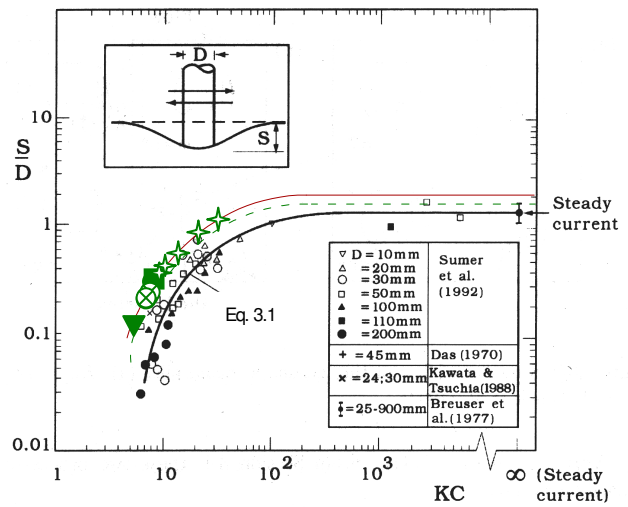
Figure 5-4: Rating of wind turbines
in the slender pile regime
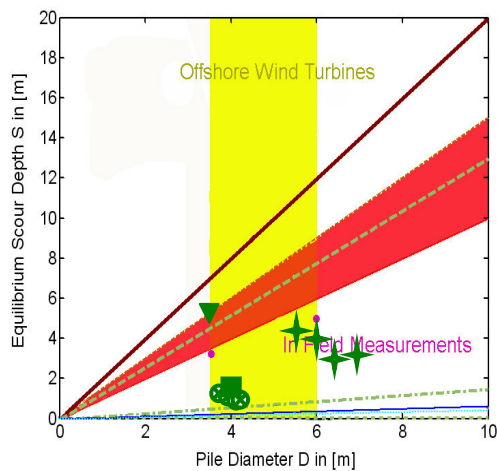
Figure 5-5: Confrontation of the maximal scour hole with design rules

None of the determined scour depth oversteps the DNV design codes. In the example of Horns Rev and EWEA the scour depth is immense overestimated by the design codes. A more detailed consideration of the maximal scour depth due to the Keulegan-Carpenter number and the possibility of breaking waves is recommendable.

5.3.2 Average scour depth

If a wind turbine is installed in a region, in which live-bed conditions are existent, the scour hole depth varies over time. In the previous subsection the maximal scour depth was determined. The conditions are expected to occur once in one hundred years. Under normal conditions the wave height is much smaller and therewith the scour hole is usually less deep. How large the difference between maximal and average scour depth is, is evaluated for the EWEA wind farm and the deep-water wind farms planned offshore the German coast.

EWEA:

Table 5-4 shows the so-called scatter diagram of the site where the EWEA wind farm is planned. The scatter diagram presents the occurrence of wave heights and their related wave periods. In this case the occurrence is given in pro mille. The second table, Table 5-5, presents the Keulegan-Carpenter number and the diffraction coefficient $^D/_L$ for the wave height and wave period combination. The grey marked fields do occur less than 0.1 ‰. The yellow fields are related to the diffraction regime. This is present in more 99% of the time. In more than 99% of the time the scour depth is beneath 30% of the pile diameter. The Keulegan-Carpenter numbers of an order of 0.1 to 0 under consideration of Figure 4-12 even indicate usual scour depths is much smaller.

Table 5-4: Scatter diagram for the EWEA location (Opti-OWECS report according to Tempel et al., 2004)

H_s in [m]	\multicolumn{8}{c}{T_z in [s]}	Sum:
	0 - 1	1 - 2	2 - 3	3 - 4	4 - 5	5 - 6	6 - 7	7 - 8	
6.5 - 7.0									
6.0 - 6.5								0.1	0.1
5.5 - 6.0							0.1	0.1	0.2
5.0 - 5.5							0.1	0.1	0.2
4.5 - 5.0							1		1
4.0 - 4.5							4		4
3.5 - 4.0						4	5		9
3.0 - 3.5						19	0.1		19.1
2.5 - 3.0					0.1	38			38.1
2.0 - 2.5					27	43			70
1.5 - 2.0				0.1	115	5			120.1
1.0 - 1.5				6	220	1			227
0.5 - 1.0				236	145	1			382
0.0 - 0.5	1		1	113	14	0.1	0.1		129.2
Sum:	1		1	355.1	521.1	111.1	10.4	0.3	1000

Table 5-5: Associated KC and $^D/_L$ of the scatter diagram for the EWEA location

H_s in [m]	KC	D/L	KC	D/L	KC	D/L	KC	D/L	KC	D/L	KC	D/L	KC	D/L	KC	D/L	Sum:
6.5 - 7.0	0.0	8.8	0.0	1.0	0.0	0.4	0.0	0.2	0.2	0.1	0.8	0.1	1.7	0.1	2.7	0.0	
6.0 - 6.5	0.0	8.8	0.0	1.0	0.0	0.4	0.0	0.2	0.2	0.1	0.8	0.1	1.6	0.1	2.5	0.0	0.1
5.5 - 6.0	0.0	8.8	0.0	1.0	0.0	0.4	0.0	0.2	0.2	0.1	0.7	0.1	1.5	0.1	2.3	0.0	0.2
5.0 - 5.5	0.0	8.8	0.0	1.0	0.0	0.4	0.0	0.2	0.2	0.1	0.6	0.1	1.3	0.1	2.1	0.0	0.2
4.5 - 5.0	0.0	8.8	0.0	1.0	0.0	0.4	0.0	0.2	0.2	0.1	0.6	0.1	1.2	0.1	1.9	0.0	1
4.0 - 4.5	0.0	8.8	0.0	1.0	0.0	0.4	0.0	0.2	0.1	0.1	0.5	0.1	1.1	0.1	1.7	0.0	4
3.5 - 4.0	0.0	8.8	0.0	1.0	0.0	0.4	0.0	0.2	0.1	0.1	0.5	0.1	0.9	0.1	1.5	0.0	9
3.0 - 3.5	0.0	8.8	0.0	1.0	0.0	0.4	0.0	0.2	0.1	0.1	0.4	0.1	0.8	0.1	1.3	0.0	19.1
2.5 - 3.0	0.0	8.8	0.0	1.0	0.0	0.4	0.0	0.2	0.1	0.1	0.3	0.1	0.7	0.1	1.1	0.0	38.1
2.0 - 2.5	0.0	8.8	0.0	1.0	0.0	0.4	0.0	0.2	0.1	0.1	0.3	0.1	0.6	0.1	0.9	0.0	70
1.5 - 2.0	0.0	8.8	0.0	1.0	0.0	0.4	0.0	0.2	0.1	0.1	0.2	0.1	0.4	0.1	0.7	0.0	120.1
1.0 - 1.5	0.0	8.8	0.0	1.0	0.0	0.4	0.0	0.2	0.0	0.1	0.2	0.1	0.3	0.1	0.5	0.0	227
0.5 - 1.0	0.0	8.8	0.0	1.0	0.0	0.4	0.0	0.2	0.0	0.1	0.1	0.1	0.2	0.1	0.3	0.0	382
0.0 - 0.5	0.0	8.8	0.0	1.0	0.0	0.4	0.0	0.2	0.0	0.1	0.0	0.1	0.1	0.1	0.1	0.0	129.2
Sum:		1				1	355.1		521.1		111.1		10.4		0.3		1000

intermediate regime: O(1) < KC < O(6)
diffraction regime: KC < O(1)

The maximal scour depth in this example was determined to be 0.3 times the pile diameter. Although it is expected, that most of the time the scour depth is much smaller due to KC ≤ 0.1, no smaller scour depth can be recommended to be considered in the fatigue analysis. This is a consequence of the lack of insight in the scour processes around large piles.

German North Sea:

As mentioned before the offshore wind turbines planned in the German North Sea show significant different conditions, so that for this example the average scour depth is evaluated as well. A scatter diagram was not available, but the 1-year maximum wave height and corresponding wave period is available (Richwien, 2004b):

Table 5-6: Prediction of the 1-year maximal scour depth for wind farm projects in the German North Sea_

h_{max} [m]	D [m]	H_{max} [m]	$T (H_{max})$ [s]	L [m]	KC [-]	D/L [-]	S/D [-]	S [m]
40.3	5	16.1	12.3	201	6.2	0.02	0.2	1.0
40.3	5.5	16.1	12.3	201	5.7	0.03	0.2	1.1
40.3	6	16.1	12.3	201	5.2	0.03	0.1	0.6
40.3	6.5	16.1	12.3	201	4.8	0.03	0.1	0.7
40.3	7	16.1	12.3	201	4.5	0.03	0.1	0.7

Theoretical the scour depth under the 1-year maximum wave conditions are about zero. Due to the including of the uncertainty effects the scour depths of 60 to 100 cm respectively 10 to 20 percent of the pile diameter are predicted. These should not be considered as the average scour depth. Most of the year the wave conditions are less severely. By a further decreasing of the Keulegan-Carpenter number the prediction of the equilibrium wave height would be 30 percent of the pile diameter. So this value is recommendable for the fatigue analysis. The recommended scour depth for the fatigue analysis is up to 66% smaller than the maximal scour depth. Hence, considering the average scour depth instead of the maximal scour depth in the fatigue analysis, the design ends up in less required steel without leading to safety risks.

Summarizing the analysis of scour at offshore wind turbines, conclusions and recommendation are given in Section 6.3.

5.4   Implication on scour protection around monopiles

The maximal loading of the scour protection around offshore wind turbines depends on the intensity of vortices (slender pile regime) as well as the intensity of diffraction (large pile regime). Under both conditions the maximal velocities due to wave and current need to be evaluated.

For slender piles reference is made to report the design of scour protection.

The theory of large piles was looked at in more detail. The cyclic loading can be determined by the MacCamy and Fuchs theory (1954). The steady loading due to the steady streaming and the current can best by evaluated of the pressure distribution theory. A simplified method was introduced: The maximal velocity of the steady streaming can be estimated as 25% of the maximal phase-resolved flow and the maximal current velocity as twice the undisturbed current velocity. The resulting loading should be determined by the summation of the shear stresses (see Section 2.2.2).

The wrong prediction of Rance (1980) as 0.75 times the pile diameter indicate, that the area is much smaller than around slender piles. This is clear from the illustration of the lee-wake vortices which extend far behind slender piles. Therewith the scour protection can be designed under consideration of the maximal scour extension at slender piles, hence 7 times the pile diameter.

6   Conclusions and Recommendations

6.1   Prediction of the maximal scour depth at large piles

Although the flow characteristics in the diffraction regime are not understood in every detail, reliable scour prediction can be made for the large pile regime and parts of the intermediate pile regime. Due to uncertainties these scour predictions are overestimating the scour depth for some conditions.

The distinctions of flow regimes by the prediction of scour depth are very important. The application in Section 5.3 showed that due to changing scour processes not necessarily the worst environmental conditions lead to the deepest scour hole. A general prediction of the maximal scour depth as presented in the Coastal Engineering Manual and in Det Norske Veritas leads to an immense overestimation of the scour potential and therewith a waste of money for steel or scour protection. Beside the flow regime also the impact of breaking waves should be evaluated for the particular case.

6.2   Scour at Offshore Wind Turbines and its consideration

The foundation piles of offshore wind turbine behave as slender piles under extreme conditions and as large piles under usual conditions.

The scour prediction for wind turbine projects showed, that with increasing diameter an overestimation of the scour depth by the design codes is made. If no wave breaking is to be expect, the limit of $S = 1 \cdot D$ is sufficient. Under breaking waves the scour can increase up to 2 times the pile diameter. Since breaking waves are not to be expected at every location, this should be evaluated for the particular location.

Under live-bed conditions the scour depth varies between the maximal scour depth and zero. The fatigue design, which was until so far mainly design driving, overestimated the stresses by assuming the maximal scour depth during the whole life time. By the application to offshore wind farms the average scour depth was estimated to be less than $S = 0.3 \cdot D$.

It is recommended to investigate the maximal scour depth in more detail. For the large pile regime only an overall prediction of the maximal scour depth was possible, however the application showed, that most of the time the Keulegan-Carpenter number is about 0.1, therewith the predicted relative scour depth of 0.3 is on the safe side, but likely much too high. The scour prediction in the diffraction regime needs to be precised. The condition under which lee-wake vortices appear combined with significant diffraction need to be investigated.

6.3   Conclusion concerning scour protection

To get the most reasonable design, a planned wind turbine must be designed with and without scour protection. By comparing the results with respect to the costs, safety and consequences of failure, the most economical design is found.

This research on scour does not result in the proof that scour protection around offshore wind turbines is a waste of money. Each individual case must be investigated. The scour depth, which needs to be considered in a design without scour protection, is in some cases much smaller than dictated in design codes. A more detailed investigation of the maximal scour hole can optimise the design. Also in the case that scour protection leads to the most economic design, detailed investigation of the flow characteristics and scoured area can optimise the design of the scour protection.

Sometimes the installation of scour protection is chosen, because the prediction of the maximal scour depth believed to be too insecure. By the investigations of this thesis uncertainties were detected in the prediction of the scour depth. However, in the design of scour protection a lot of insecurities exist as well (maximum design load, filter, installation inaccuracies). The installation of scour protection as a consequence of uncertainties is unreasonable.

The observation of foundations with and without scour protections is strongly recommended. Monitoring counteracts the uncertainties in the design and provides valuable data for the improvement of scour prediction and scour protection.

For monopile-founded offshore wind turbines the scour protection need to be designed according to "slender" piles, since under extreme conditions the pile is classified as slender. The design of scour protection was not a main objective of this investigation, nor the scour around slender piles, so that no conclusions to improve the design of scour protection are drawn.

6.4   Shortcomings in this research and further research

Predictions of scour depth according to model tests were found, but the application on offshore wind farm designs is not clear. Beside the common uncertainties, scour around offshore wind turbines can be enlarged by the motion of the pile. Model tests in this field are needed. The estimation of uncertainties should be verified.

The prediction of a maximal scour depth due to diffraction was validated to be much smaller than around slender piles. Predictions were made for wave, wave and current and offshore wind turbines. Investigations of models as well as improvement of analytical computer models are recommendable to precise the scour prediction in the large and intermediate pile regime.

A lot can be learned from in field measurement especially since permanent monitoring techniques were developed. Parallel measurements of wave and current conditions should be performed. These measurements are expensive, but monitoring is necessary around the foundations of wind turbines anyway, because the scour prediction as well as the design of scour protection shows uncertainties.

References

Chapter 1

Cockerill, T.T., Harrison, R., Kühn, M., van Bussel, G.J.W. (1997):"Comparison of Cost of Offshore Wind Energy at European Sites", Opti-OWECS, Vol.3

Breusers, H.N.C., Nicollet, G., Shen, H.W. (1977):" Local scour around cylindrical piles", J. Hyd. Res., vol. 15, p.211-252

DNV, Det Norske Veritas, Offshore standard DNV-OS-J101, "Design of Offshore Wind Turbine Structures", Draft 20040212

Katsui, H., Toue, T.(1993): „Methodology of estimation of scouring around large-scale offshore structures", Proc. 3rd Int. Offshore and Polar Eng. Conf., Vol. I, p.599-602

Rance, P.C. (1980): "The potential of scour around large objects" in "Scour Prevention Techniques Around Offshore Structures", Society for Underwater Technology, London, p. 41-53

Saito, E., Sato, S., Shibayama, T. (1990): "Local Scour around a Large Circular Cylinder due to Wave Action". Proc. 22nd Int Conf. Coastal Engineering, Delft, Netherlands, Chapter 134

Sumer, B.M., Fredsoe, J., Christiansen, N. (1992): "Scour around a vertical pile in waves", J. Waterway, Port, Coastal and Ocean Eng., ASCE, vol. 117, p.15-31

Tempel, J. van der, Zaaijer, M.B., Subroto, H. (2004): "The Effects of Scour on the Design of Offshore Wind Turbines", Report at TU Delft

Ungruh, G., Zielke, W.(2003): "Kolkberechnung an Offshore-Bauwerken: a state of the art review", Uni Hanover, www.hydromech.uni-hannover.de/Mitarbeiter/MDORF/Gigawind2/papers.html

Van der Oord ACZ B.V.(2003):"Scour protection for 6MW OWEC with monopile foundation in North Sea", www.ecn.nl/docs/dowec/10050_001.pdf

Coastal Engineering Manual (2003):"EM 1110-2-1100 (Part VI)", Chapter 5, p.242-245, Washington

Zaaijer, M.B. (2004a): Slides of Offshore Wind Farm Design, "Introduction", TU-Delft

Chapter 2

Bladed Version 3.51, Garrad Hassan and Partners Ltd., Bristol

Dessens, M. (2004): "The Influence of Flow Acceleration on Stone Stability", Master thesis, TU   Delft, Faculty of civil engineering, Hydraulic Engineering Section (www.waterbouw.tudelft.nl → education → MSc theses)

DNV, Det Norske Veritas, Offshore standard DNV-OS-J101, "Design of Offshore Wind Turbine Structures", Draft 20040212

Fredsøe, J., Deigaard, R. (1992): "Mechanics of Coastal Sediment transport", Singapore

Hoffmans, G.J.C.M., Verheij, H.J. (1997): "Scour Manual", Rotterdam

Kirchner, J.W. (1990): "Gaia metaphor unfalsifiable", Nature, p.345-470

LIMAS (Liquefaction Around Marine Structures) (2004):
    http://vb.mek.dtu.dk/research/limas/limas.html

Oumeraci, H. (1996):"Wellentransformation", Vorlesungsskript, TU-Braunschweig, Germany

Schaumann, P., Kleineidam, P., Wilke, F. (2004): "Fatigue Design bei Offshore-Windturbinen", Stahlbau 73, p.716-726, Germany

Shields, A. (1936): "Anwendung der Ähnlichkeitsmechanik und der Turbulenzforschung auf die Geschiebebewegung" Mitteilung der Preußischen Versuchsanstalt für Wasserbau und Schiffbau, Berlin, Heft 26

Sleath, J.F.A. (1978): "Measurements of bed load in oscillatory flow", J. Waterway, Port, Coastal and Ocean Eng., p.291-307

Sumer, B.M., Fredsøe, J. (1997): "Hydrodynamics around Cylindrical Structures", Singapore

Sumer, B.M., Fredsøe, J. (2002): "The Mechanics of Scour in the Marine Environment", Singapore

Swart, H. (1976): "Predictive equations regarding coastal transport", Proc. 15th conference on coastal engineering, Honolulu

Tempel, J. van der, Zaaijer, M.B., Subroto, H. (2004): "The Effects of Scour on the Design of Offshore Wind Turbines", Report at TU Delft

Terrile, E. (2004): "The Threshold of Motion of Coarse Sediment Particles by Regular Non-Breaking Waves", master thesis, TU Delft (www.waterbouw.tudelft.nl → education → MSc theses)

Tromp, M. (2004): "Influence of Fluid Acceleration on the Threshold of Motion" , Master thesis, TU Delft, (www.waterbouw.tudelft.nl → education → MSc theses)

Whitehouse, R.J.S. (1998): "Scour at Marine Structures", London

Zaaijer, M.B. (2004b): Slides of "Offshore Wind Farm Design, "Dynamics", TU Delft

Zhao, M., Teng, B., Li, L.: "Local Scour around a Large-Scale Vertical Circular Cylinder due to Combined Wave-Current Action", Journal of Hydrodynamics (China), Ser. B, 1(2004),p.7-16

Chapter 3

Bijker, E.W., Asce, M., de Bruyn, C.A. (1988): "Erosion around a pile due to current and breaking waves", Int. Conf. Coastal Engineering, Vol.2, Malaga, Spain

Breusers, H.N.C., Nicollet, G., Shen, H.W. (1977):" Local scour around cylindrical piles", J. Hyd. Res., vol. 15, p.211-252

Halfschepel, R. (2001): "Consept study bottom protection around pile foundation of 3 MW turbine, Doc. No. 23, Van Oord ACZ B.V.

Hoffmans, G.J.C.M., Verheij, H.J. (1997): "Scour Manual", Rotterdam

Ungruh, G., Zielke, W.(2003): "Kolkberechnung an Offshore-Bauwerken: a state of the art review", Uni Hanover,
www.hydromech.uni-hannover.de/Mitarbeiter/MDORF/Gigawind2/papers.html

Sumer, B.M., Fredsoe, J., Christiansen, N. (1992): "Scour around a vertical pile in waves", J. Waterway, Port, Coastal and Ocean Eng., ASCE, vol. 117, p.15-31

Sumer, B.M., Fredose, J. (2001a): "Scour around a pile by combined wave and current", J. Hydraulic Eng., ASCE, Vol. 127, p.403-411

Sumer, B.M., Fredsøe, J. (2002): "The Mechanics of Scour in the Marine Environment", Singapore

Sumer, B.M., Whitehouse, R.J.S., Tørum, A. (2001a):"Scour around coastal structures: a summary of recent research", Coastal Engineering, p.153-190

Ungruh, G., Zielke, W.(2003): "Kolkberechnung an Offshore-Bauwerken: a state of the art review", Uni Hanover,
www.hydromech.uni-hannover.de/Mitarbeiter/MDORF/Gigawind2/papers.html

Whitehouse, R.J.S. (1998): "Scour at Marine Structures", London

Chapter 4

Daugherty, R.L., Franzini, J.B., Finnemore, E.J.: "Fluid Mechanics with Engineering Applications", 8th Edition New York 1985

Fredsøe, J., Deigaard, R. (1992): "Mechanics of Coastal Sediment transport", Singapore

Hoffmans, G.J.C.M., Verheij, H.J. (1997): "Scour Manual", Rotterdam

Katsui, H., Toue, T.(1993): „Methodology of estimation of scouring around large-scale offshore structures", Proc. 3rd Int. Offshore and Polar Eng. Conf., Vol. I, p.599-602

Kobayashi, T.: "3-D Analysis of Flow around a Vertical Cylinder on a Scoured Bed", Intern. Conf. on Coastal Engineering, Proc. 23rd, Venice, Italy 1994, vol.3 p.3482-3495

Kobus, H. (1978): "Wasserbauliches Versuchswesen", Deutscher Verband für Wasserwirtschaft (DVWW)"

MacCamy, R.C., Fuchs, R.A. (1954): "Wave forces on piles: A diffraction theory", U.S. Army Corps of Engineers, Beach Erosion Board, Tech. Memo No. 69, p.17

May, R.P., Willoughby, I.R. (1990): "Local Scour around large obstructions", HR Wallington Report SR 240

Oumeraci, H. (1996):"Wellentransformation", Vorlesungsskript, TU-Braunschweig, Germany

Nielson, P., Callaghan, D.P. (2002): "Shear Stress and Sediment Transport Calculations for Sheet Flow under Waves", Coastal Engineering Journal (No. 47, p. 347-354)

Rance, P.C. (1980): "The potential of scour around large objects" in "Scour Prevention Techniques Around Offshore Structures", Society for Underwater Technology, London, p. 41-53

Saito, E., Sato, S., Shibayama, T. (1990): "Local Scour around a Large Circular Cylinder due to Wave Action". Proc. 22nd Int Conf. Coastal Engineering, Delft, Netherlands, Chapter 134

Saito, E., Shibayama, T. (1992): "Local Scour around a Large Circular Cylinder on the Uniform Bottom Slope due to Waves and Currents", Proc. 23rd Inf. Conf. Coastal Engineering, Venice, Italy, p.2799-2810

Sumer, B.M., Fredsøe, J. (1997): "Scour around a Large Vertical Circular Cylinder in Waves", Proc. 16th Intern. Offshore and Artic Eng. Conf., Yokohama, p.13-18

Sumer, B.M., Fredsøe, J. (2000): "Experimental study of 2D scour and its protection at a rubble-mound breakwater", Coastal Engineering, vol. 40, p.59-87

Sumer, B.M., Fredsøe, J. (2001b): "Wave Scour around a Large Vertical Circular Cylinder", Journal of Waterway, Port, Coastal and Ocean Engineering

Sumer, B.M., Whitehouse R.J.S., Tørum, A.: "Scour around Coastal Structures: a Summary of Recent Research", Coastal Engineering 44(2001) p.153-190

Toue, T., Katsui, H., Nadaoka, K.(1992): "Mechanism of Sediment Transport around a Large Circular Cylinder", Pro. 23rd Int. Conf. of Coastal Engineering, Venice, Italy, 219 p. 2867-2878

Whitehouse, R.J.S. (1998): "Scour at Marine Structures", London

Zhao, M., Teng, B., Li, L.: "Local Scour around a Large-Scale Vertical Circular Cylinder due to Combined Wave-Current Action", Journal of Hydrodynamics (China), Ser. B, 1(2004),p.7-16

BSH (2004): "Jahresbericht der Bundesanstalt für Seeschifffahrt und Hydrographie" www.bsh.de/de/Produkte/Infomaterial/Jahresbericht-2004/Jahresbericht 2004kompakt.pdf#

Richwien, W., Lesny, K. (2004b): "Windfarmen in der Nordsee" Essener Unikate, Heft 23, p. 60-69, Essen

Chapter 5

Ferguson, M.C., Kühn, M.m., Bierbooms, W.A., Cockeril, T.T., Göransson, B., Harland, L.A., van Bussel, G.J.W., Vugts, J.H., Hes, R.(1998): "A Typical Design Solution for an OWECS",Opti Owecs, Vol. 4

Richwien, W., Lesny, K. (2004a): "Kann man Kolke an Offshore-Windenergieanlagen berechnen?",
www.hydromech.uni-hannover.de/Mitarbeiter/MDORF/Gigawind2/papers.html

Richwien, W., Lesny, K. (2004b): "Windfarmen in der Nordsee" Essener Unikate, Heft 23, p. 60-69, Essen

www.ewea.org

www.ilr.tu-berlin.de/WKA/windfarm/offshore.html

www.londonarray.com

www.windenergynews.blogspot.com

Appendices

Appendix A

Definition of Parameters

Definition of Reynolds number   (Re):

Original definition:

Osborne Reynolds (1842 -1912) defined the Reynolds number in 1883 as criterion to describe the turn over of laminar to turbulent flow regime by

$$Re = \frac{vD_L}{\nu} \qquad (1)$$

(according to Oumeraci, 1996)

with D_L : clear diameter of pipeline
     v : velocity
     υ : viscosity

For a flow with a Reynold number smaller Re_{crit} ($\approx$ 10.000) a disturbance will abate back to a laminar flow regime, in a flow with a Reynolds number higher than Re_{crit} a disturbance will cause a turbulent flow regime. The Reynolds number is an important parameter for flows of liquid as well as of gases.
Beside the distinction between laminar and turbulent flow, it is an important indicator of dynamic similarity and a value to determine the drag-resistant of a flow.

Flow around structures:

$$Re = \frac{uD}{\nu} \qquad (2)$$

with   D := Pile diameter
     u := velocity

$Re_{crit} = 3*10^5 - 5*10^5$

(according to Sumer and Fredsoe, 2002)

Bed-boundary layer:

$$Re_\delta = \frac{u\delta}{\nu} \qquad (3)$$

with δ := height of bed boundary layer

$Re_{crit} = 1.5*10^5$

(accoding to Fredsoe and Deigaard,1992)

Particle Reynolds number:

$$Re_* = \frac{u_{*c}d}{\upsilon} \qquad (4)$$

with d : stone diameter
     ν : kinematic viscosity

Defintion of the Keulegan-Carpenter Number (KC):

The Keulegan-Carpenter number is a dimensionless parameter to relate the motion of water particles under waves to the diameter of a flowed pile or structure.

$$KC = \frac{U_m T_w}{D} \approx \frac{2\pi a}{D} = \frac{2\pi}{D} \frac{H}{2} \frac{1}{\sinh(kh)}$$
(5)

KC : Keulegan-Carpenter number   [-]
U_m : maximal velocity of the flow   [m/s]
T_w : period of the wave motion   [s]
D : cylinder diameter   [m]
a   : amplitude of the orbital motion at the sea bed   [m]
H : wave height   [m]
k   : wave number   [1/m]
h   : water depth   [m]

As can be interpreted out of Eq. (5), a small Keulegan-Carpenter number is an index for a relative small orbital motion relative to the pile diameter. Further a small KC relates to a thin boundary layer (Whitehouse) in respect to the pile diameter.
KC is a characteristic parameter for the flow regime around a pile as well as the equilibrium scour depth.
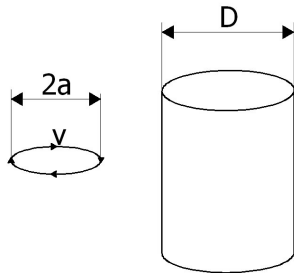

Figure 1: Illustration of KC

In Section 2.1 it is stated that important boundaries for the occurrence of flow separation and formation of vortices are KC = O(1) and KC = O(6) as follows:

KC = O(1): The circumference of the ellipse is as large as the pile diameter
KC < O(1): The circumference of the orbital motion is smaller than the diameter of the pile

KC = O(6): The horizontal amplitude of the orbital motion is approximately as large as the pile diameter.
KC < O(6): The horizontal amplitude of the orbital motion is smaller than the pile diameter.

Defintion of Froude:

$$Fr = \frac{u}{\sqrt{gh}} \begin{cases} < sub-critical \\ = critical \\ > super-critical \end{cases} \tag{6}$$

Fr is the coefficient which relates inertial to gravitational forces or kinetic versus potential flow. A high Froude number Fr indicates a high flow velocity and a high scour potential. Originally the Froude number was a parameter to describe the flow in a free open channel flow.

Appendix B

Definition of the Boundary Layer

Boundary layer:

The region in which the presence of a wall (sea bed, pile) influences the flow is called boundary layer. At the "boundary" the velocity need to be zero. The velocity distribution can have different shapes. In Figure 2 a logarithmic velocity distribution of a bed boundary layer is shown.
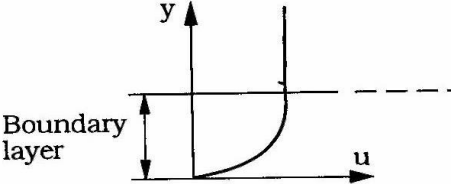

Figure 2: Bed-boundary layer with logarithmic velocity distribution (Sumer and Fredsoe, 1997)

A logarithmic velocity distribution occurs in stationary uniform flows. The velocity distribution in an accelerated flow has a different shape which is not researched well. In Figure 3 the velocity distribution in the bed-boundary layer under waves is shown.
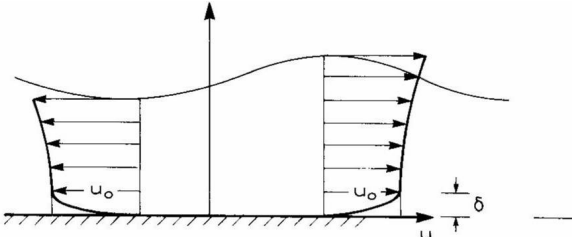

Figure 3: Bed-boundary layer under real waves (Fredsoe and Deigaard, 1992)

The height of the boundary layer can be estimated by Eq. (6) from Booij (1992):

$$d\delta/dt = \kappa\, u_* \approx 0.4\, u_*$$

with κ : Karman constant [-]
          $u_* \approx 0.1\, u_b$
          u_b : near bed velocity [m/s]

The height of the bed-boundary layer and the velocity distribution depend on the bed roughness which is difficult to predict.

Appendix C

Equilibrium Scour Hole at Large Piles
by Sumer and Fredsøe (2002)

Equilibrium Scour Depth at Large Cylinders
by Sumer and Fredsøe

Given:

D   : diameter of the cylinder
d_{50} : medium diameter of the sand
T_w : wave period
H   : wave height
h   : water depth

1. Calculate deep-water wave length by

$$L_0 = \frac{gT_w^2}{2\pi}$$

and the wave length

$$L = L_0 \tanh (kh)$$

2. Determine the coefficient h/L_0 and determine therewith the sinusoidal wave with the help of wave tables. *(The same solution can be acchieved by calculating with Airy wave theory.)*

➔ $\sinh(kh)$ for H/L_0

3. Calculate the amplitude of the orbital motion of the water particles at the seabed assuming the linear wave theory

$$\eta = \frac{H}{2}\frac{\cosh(k(z+h))}{\sinh(kh)} = \frac{H}{2}\frac{1}{\sin(kh)}$$

and the maximal velocity at the bed

$$u_{max} = \frac{\pi H}{T}\frac{\cosh(k(z+h))}{\sinh(kh)}$$

4. Check the sinusoidal theory by determining the Ursell parameter:

$$U = \frac{HL^2}{h^3} < 15$$

If the Ursell parameter is smaller than 15 the sinusoidal theory might be applied, otherwise the cnoidal theory is recommended.

5. Calculate the scour parameters KC and $^D/_L$

$$KC = \frac{2\pi a}{D}$$

6. Using the table of Sumer and Fredsøe given in Figure 4-13 the scour coefficient S/D can be estimated and therewith the maximum scour depth is easily calculated.
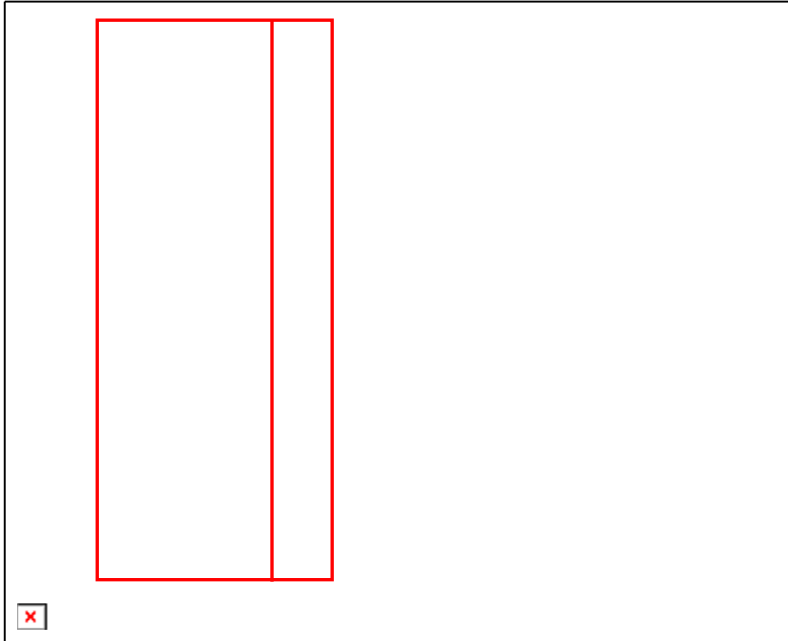
S/D → S

Figure 4-13: Prediction of the equilibrium scour depth by Sumer and Fredsøe (2002)

7. Since Figure 4-13 is only valid for live-bed scour, this assumption needs to be checked:

Shields parameter: $\theta = \dfrac{U_f m^2}{g(s-1)d} = \dfrac{\frac{f_w}{2} U_m^2}{g(s-1)d}$

with $\quad f_w = 0.035 Re^{-0.16} \quad \approx 0.003$ (Fredsoe and Deigaard, 1992)

Appendix D

MacCamy and Fuchs theory (1954)

MacCamy and Fuchs theory

The McCamy and Fuchs theory is an application of the linear diffraction theory on circular piles. The velocity potential function is determined by the summation of the incident-wave potential function and scattered-wave potential function. The scattered-wave field is related to the reflected waves and diffracted waves.

The following boundary conditions are considered:
- the vertical velocity at the bed is zero
- the pressure at the free surface is constant
- the normal velocity at the surface of the pile is zero

The Bessel function and the Hankel function are included in the progressing software "Matlab".

Velocity potential:

$$\phi = -i\frac{gH}{2\omega}\frac{cosh(k(z+h))}{cosh(kh)}\sum_{p=0}^{\infty}\varepsilon_p i^p\left[J_p(kr) - \frac{J_p'(kr_0)}{H_p^{(1)'}(kr_0)}H_p^{(1)}(kr)\right]\cos(p\theta)e^{-i\omega t}$$

with $J_0(kr) = 1 + \sum_{n=1}^{\infty}\frac{(-1)^n(kr)^{2n}}{2^{2n}(n!)^2}$ (Bessel function of order zero)

$$J_1(kr) = \frac{kr}{2}\sum_{m=0}^{\infty}\frac{(-1)^m(kr)^{2m}}{2^{2m}(m+1)!m!}$$

(Hankel function)

$$H_p^{(1)} = J_p(kr) + iY_p(kr)$$

with $Y_0(kr) = \frac{2}{\pi}\left[(\gamma + ln\frac{kr}{2})J_0(kr) + \sum_{m=1}^{\infty}\frac{(-1)^{m+1}h_m}{2^{2m}(m!)^2}(kr)^{2m}\right]$ (Bessel function of order 1)
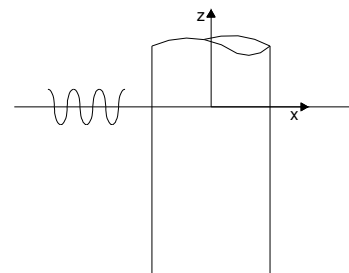
$$Y_1(kr) = \frac{2}{\pi}[-y_2(kr) + \gamma - ln2)J_1(kr)]$$

$$y_2(kr) = -J_1(kr)ln(kr) + \frac{1}{kr}\left[1 - \sum_{m-1}^{\infty}\frac{(-1)^m(H_m + H_{m-1})}{2^{2m}m!(m-1)!)}(kr)^{2m}\right]$$

$$\gamma \cong 0.5772$$

$$h_m = \frac{1}{m} + \frac{1}{m-1} + \frac{1}{m-2} + ... + 1$$

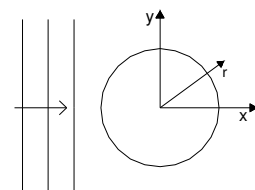Φ = velocity potential
r_0 = diameter of the pile
ε_m unity for $m = 0$ and 2 for otherwise
k = wave number
ω = angular wave frequency

Velocities in plan:

$$u_r = -\frac{\partial\phi}{\partial r} \qquad u_\theta = -\frac{1}{r}\frac{\partial\phi}{\partial\theta}$$

$$u_{plain} = \sqrt{u_r^2 + u_\theta^2}$$

Appendix E

Confrontation of the prediction and in field measurements

[data taken from http://www.golfklimaat.nl/]

Europlatform (52° N, 3.3 °E)

water depth h = 32 m,
pile diameter D = 3.5 meter

The pile diameter is similar to those form wind turbines, the water depth is about 10 meter deeper. Therewith the resulting KC is smaller than at wind turbines.

wave height: H_{m0} = 6.8 m H_{m0} (in 100 years)

H_{m0} = 4 *sqrt(m0)
H1/3 = 0.95 * H_{m0}
Hmax = 1.86 * H1/3 = 12m

L_{max} = 3.7 * $(H_{max})^2$ = 532.8m   (for North Sea conditions, according to Zaaijer (2004))

KC = 2 π a/D = π H/D * $(sinh(kh))^{-1}$ = 28

By the equation (3.1) of Sumer et al. (1992) the equilibrium scour depth is determined to be 3.33m. The measured scour depth was 3 meter. Since it is likely, that the once-in-100-years wave height was not reached and the measurement might have taken place shortly after the storm, the results fit well.

Schiermonnikoog

h = 7m
D = 6m

The conditions are not similar to those from wind turbines, but this example is a proof for the theory of scouring.

H_{m0} = 8.59 m
H_{max} = 1.86 * 0.95 * H_{m0} = 15.2

wave breaking occur if $(^H/_L)_{max}$ = $^1/_7 \cdot$ tanh (kh)   or $(H/h)_{max}$ = 0.6 to 1.2

from $(H/h)_{max}$ $\rightarrow$ H_{max} = 8.4m, the maximal wave height of 15.2 meters can not occur. The measured waves of 8.59 meters are breaking, which leads to an increase of the maximal scour depth.

T = 10.4 to 16.6 s (Tm-1, Tm02, Tp)   (www.golfklimaat.nl)

by L = L_0 * tanh(kh) the wave length differ between 169 meter and 430 meter. This is too loose, to determine the scour depth. The calculated Keulegan-Carpenter number differs between 0.08 and 15.

The measured scour depth was 4.8 meters or 0.8 times the diameter.

Appendix F

Example Application to Offshore Wind Turbines

a)   Horns Rev (Denmark, 2002):

The wind farm Horns Rev is the largest built offshore wind farm. It consists out of 80 turbines and is located 14 to 20 km offshore the west coast of Denmark in the North Sea. The turbines are constructed on drilled piles with a diameter of 4 meter. Evaluating the maximal water depth of 14 meters and the maximal wave height of 8 meters (with a period of 7s), the Keulegan-Carpenter number is determined to be 8.7. Therewith these turbines are founded on slender piles. By the scour prediction of Sumer et al. (1992) (Eq. 3.1) the equilibrium scour depth will be less than 0.2 times the pile diameter.

b)   Blyth (UK., 2000):

Two wind turbines have been installed on drilled monopiles one kilometre from shore near Blyth in the north of England. The pile diameters are 3 meters, the maximal water depth is 8.5 meters, the maximal wave height is 8 meters with a period of 7 seconds. The Keulegan-Carpenter number results in 5.7. This is a bit smaller than the regime boundary of KC = 6, even so the scour should be analysed as slender pile regime. Since the diffraction coefficient $^D/_L$ is 0.07, the lee-vortices dominate the scour process and not the diffraction. By Sumer et al. (1992) the equilibrium scour depth for KC = 6 results in zero. But the design by Sumer et al. (1992) would underestimate the scour. Considering the wave steepness $(H/L)_{max}$ (see Section 2.1.3), breaking waves will occur. A scour depth of more than 1 time of the diameter is imaginable.

c)   Egmond aan Zee (The Netherlands, until 2006)

Some weeks ago the final contract for a large scale wind farm at the coast of the Netherlands was signed. 36 turbines are to be installed near shore in the North Sea. In the area the water depth is up to 20 meters deep. A maximal wave height of 8.1 meter is expected with a period of 7 seconds. In literature (Tempel et al., 2004; www.windenergynews.com) the preliminary diameter of 3.5 meters was published. This seems small in comparison with the conditions of Horns Rev, where the water depth and wave height is smaller, but the pile diameter larger.

For the diameter of 3.5 meters the Keulegan-Carpenter number is 8.5. For a larger diameter of 4 meters like in Horns Rev, where the maximal water depth and the maximal wave height are smaller, the Keulegan-Carpenter number would be 7.4. Again the scour depth must be evaluated by the slender-pile theory. By the modified prediction based on Sumer et al. (1992) the maximum scour depth around the 3.5 meter large pile is 0.3 times the pile diameter (= 105 centimetres). For the pile diameter of 4 meters the scour depth to pile diameter ratio according to Sumer et al. (1992) is 0.4 which equals a maximal scour depth of 160 centimetres.

d)   German Wind Farm Projects in the North Sea:

Germany plans a lot of offshore wind farms. Their conditions are different than common wind farms. The locations show mean water depth of about 30 meters. Under extreme conditions up to 40.3 meters. This is about twice as high as at existing wind turbines. The prognosticated maximal wave height of 23.3 meters (once-in-50-years) with a related wave period of 14.5 seconds is also much higher than at "usual" offshore turbines. Thereby pile diameters of 4 meter are not sufficient. Considering pile diameters of 5 to 7 meters, the Keulegan-Carpenter number is calculated as 9 to 12. Under extreme conditions even these large piles behave as slender piles. The determined maximal scour depth by the modified prediction of Sumer et al. (1992) vary between once the diameter around a pile with a diameter of 5 meter and 40% of the pile diameter around a 7 meter large pile.

Eidesstattliche Erklärung

Ich erkläre hiermit an Eides Statt, dass ich die vorstehende Diplomarbeit selbständig angefertigt und die benutzten Hilfsmittel sowie die befragten Personen und Institutionen vollständig angegeben habe.

Braunschweig, den

(Unterschrift mit Vor- und Zunamen)